Optimal internal dissipation of a damped wave equation using a topological approach

Arnaud Münch*

August 2, 2008

Abstract

We consider a linear damped wave equation defined on a bi-dimensional domain Ω, with a dissipative term localized on the subset ω. We address in this work the shape design problem which consists in optimizing the shape of ω in order to minimize the energy of the system at a given time T. By introducing an adjoint problem, we first obtain explicitly the (shape) derivative of the energy at time T with respect to the variation of ω. Expressed as a boundary integral on $\partial\omega$, this derivative is then used as an advection velocity in an Hamilton-Jacobi equation for changing the shape. We use the level-set methodology on a fixed working Eulerian mesh as well as the topological derivative notion. We also consider the optimization with respect to the value of the damping parameter. The numerical approximation is presented in details and several numerical experiments are performed and relate the over-damping phenomenon to the well-posedness of the problem.

Key Words: Shape design, wave equation, level set, topological derivative, numerical viscosity.

Mathematics Subject Classification (2000): 49J45, 65N30.

1 Introduction - Problem statement

Let $T > 0$ and Ω a bounded domain of class $C^2(\mathbb{R}^2)$. We consider the standard damped wave equation on the cylinder:

$$\left\{\begin{array}{ll} y''_{\omega,a} - \Delta y_{\omega,a} + a(\boldsymbol{x})y'_{\omega,a} = 0 & \text{in } \Omega\times(0,T), \\ y_{\omega,a} = 0 & \text{on } \partial\Omega\times(0,T), \\ y_{\omega,a}(\boldsymbol{x},0) = y_0(\boldsymbol{x}), \quad y'_{\omega,a}(\boldsymbol{x},0) = y_1(\boldsymbol{x}) & \text{in } \Omega. \end{array}\right. \tag{1}$$

where the symbol $'$ denotes partial differentiation with respect to time. We assume that the damping potential $a \in L^\infty(\Omega,\mathbb{R}^+)$ takes the expression

$$a(\boldsymbol{x}) = a\mathcal{X}_\omega(\boldsymbol{x}) \quad \forall \boldsymbol{x}\in\Omega \tag{2}$$

for any $a \in \mathbb{R}^+$. $\mathcal{X}_\omega$ designates the characteristic function of any domain ω strictly included in Ω. Moreover, we assume that $(y_0, y_1) \in (H^2(\Omega)\cap H_0^1(\Omega))\times H_0^1(\Omega)$ are independent of ω and a. System (1) is well-posed (see [19]) and the unique solution satisfies

$$y_{\omega,a} \in C((0,T);H^2(\Omega)\cap H_0^1(\Omega))\cap C^1((0,T);H_0^1(\Omega))\cap C^2((0,T);L^2(\Omega)). \tag{3}$$

*Laboratoire de Mathématiques de Besançon, Université de Franche-Comté, UMR CNRS 6623, 16, route de Gray 25030 Besançon, France - arnaud.munch@univ-fcomte.fr. Partially supported by grants ANR-05-JC-0182-01 and ANR-07-JC-1832-84.

The energy of the system (1)

$$E(\omega, a, t) = \frac{1}{2}\int_\Omega (|y'_{\omega,a}(\boldsymbol{x}, t)|^2 + |\nabla y_{\omega,a}(\boldsymbol{x}, t)|^2)dx, \quad \forall\ t > 0, \tag{4}$$

satisfies the following dissipation law

$$E'(\omega, a, t) = -\int_\Omega a(\boldsymbol{x})|y'_{\omega,a}(\boldsymbol{x}, t)|^2 dx \leq 0, \quad \forall t > 0. \tag{5}$$

so that the linear wave equation (1) models the dissipation of a membrane by an internal actuator. $y_{\omega,a}(\boldsymbol{x}, t)$ denotes the transversal displacement at point $\boldsymbol{x}$ and time t, while y_0 and y_1 denote the initial position and the velocity respectively.

In this work, we consider the numerical resolution of the following nonlinear problems

$$(P_\omega) : \inf_{\omega\in\Omega} E(\omega, a, T) \quad ; \qquad (P_a) : \inf_{a\in L^\infty(\Omega,\mathbb{R}^+)} E(\omega, a, T). \tag{6}$$

Problem (P_ω) - illustrated on Figure 1 - is a so-called shape design problem and consists in optimizing the dissipation of the system at time T with respect to ω. This a typical ill-posed problem in the sense that the infimum may be not reached in the class of characteristic function: the optimal domain ω is then composed of an arbitrarily large number of disjoint components. In [25] (extended to the elasticity operator in [26]), a full well-posed relaxation of (P_ω) is given, using a non-convex variational analysis (we also refer to [11] for an analysis in the 1-D case). The analysis performed in [25] highlights the effect of the overdamping phenomenon characteristic to this damped wave equation ([12, 20]), for which the dissipation vanishes for large value of the constant a: precisely, (P_ω) loose his well-posedness as soon as this constant is large enough (with respect to the data of the problem). This observation motivates the numerical resolution of problem (P_a), not studied so far in the general case (in the 1-D case, we refer to [12]).

We highlight, that in this work, we do not make any geometrical assumption on ω (contrary to [15, 16] which maximize the exponential decay rate of the energy with respect to ω, assuming the optic geometrical condition, well-known in control theory [4]).

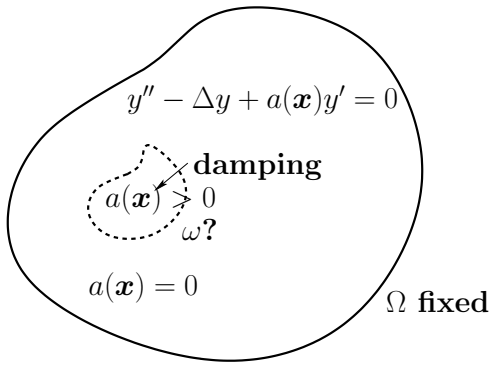

Figure 1: Illustration of (P_ω) - Optimization of the location and shape of ω, support of the damping function a in order to minimize the energy E at time T.

This paper provides a numerical solution to the nonlinear problems (6) in order to complete the previous theoretical work [25]. Provided some additional geometrical conditions on the ω, observe that problem (P_ω) is well-posed [18]. In order to use a gradient descent algorithm, a key point is to determine the derivative of E with respect to ω and a. This is done using the domain derivative method [9]: the derivative with respect to ω is expressed

as a curvilinear integral over $\Gamma = \partial\omega \times (0,T)$ and is a function of $y_{\omega,a}$ and $p_{\omega,a}$ solution of an adjoint problem and the jump of a across $\partial\omega$. The derivative with respect to a, expressed on $\omega \times (0,T)$ is also function of $p_{\omega,a}$. Then, the optimal shape design problem (P_ω) is addressed with a level set approach, following the recent works [1, 31] (see [5] for a survey on this question). From a numerical viewpoint, we discuss the approximation of the wave equation in such a way that the spurious high frequencies get damped out uniformly with respect to the discretization parameters. In order to ensure the convergence of the derivative of the energy derivative (which is necessary for the convergence of the discrete optimal design), we use a modified scheme with viscosity terms introduced and analyzed in [24].

The paper is organized as follows. The next section is devoted to the computation of the (shape) derivative of E with respect to the variation of ω and also with respect to the damping function. Section 3 aims at recalling some aspects of level set methods and presents the algorithm of minimization. Section 4 is devoted to the numerical approximation of the problem using a modified finite difference scheme. Section 5 presents several numerical simulations of problems (P_ω), (P_a) and also of problem $(P_{\omega,a})$ which consists of minimizing the energy which respect to ω and a simultaneously. We conclude with some remarks in Section 6.

2 Existence results and derivative of E

2.1 Overview of existence results for (P_ω) and (P_a)

The aim of this part is to recall some assumptions which ensure the existence of at least one solution to problems (P_ω) and (P_a). Let us first make the following important remarks.

Remark 1 *We underline that no condition is imposed on $\partial\omega$. This will allow us to use the level set approach which consists of decoupling the description of the moving boundary $\partial\omega$ from the description of the mesh of Ω. It is also important to notice that, in the case where $a \in L^\infty(\Omega)$, the unique solution y of (1) is such that ∇y is continuous on and through $\partial\omega$. Precisely, we recall that when $\Omega = (\Omega\backslash\omega) \cup \omega \cup \partial\omega$, then*

$$H^1(\Omega) = \{v \in L^2(\Omega), v_{|\omega} \in H^1(\omega), v_{|(\Omega\backslash\omega)} \in H^1(\Omega\backslash\omega), [[v]] = 0 \text{ on } \partial\omega\} \tag{7}$$

where $[[v]]$ denotes the jump of v through $\partial\omega$. Then, the interpretation of the following variational formulation associated with (1), for all $\varphi \in \mathcal{D}(\Omega)$ and for all $t > 0$,

$$< y''_{\omega,a}, \varphi >_{(H^{-1}(\Omega),H_0^1(\Omega))} + \int_\Omega \nabla y_{\omega,a}.\nabla\varphi dx + \int_\omega a y'_{\omega,a}\varphi dx = 0 \tag{8}$$

implies using the density of $\mathcal{D}(\Omega)$ in $H_0^1(\Omega)$ that $\int_{\partial\omega}[[\nabla y_{\omega,a}\cdot\boldsymbol{\nu}]]\varphi d\sigma = 0$ for all $\varphi \in H^{1/2}(\partial\omega)$ and finally $[[\nabla y_{\omega,a}\cdot\boldsymbol{\nu}]] = 0$. Then, $[[y_{\omega,a}]] = 0$ implies $[[\nabla y_{\omega,a}.\boldsymbol{\tau}]] = 0$. ■

Remark 2 *The energy E at time T - called the cost function in the sequel - is not monotonous with respect to the area of ω. Moreover, without any restriction on the area of ω, one may conjecture that the trivial solution is $\omega = \Omega$. Similarly, one may conjecture that the inclusion $\omega_1 \subset \omega_2 \subset \Omega$ implies the inequality $E(\omega_2, a, T) \leq E(\omega_1, a, T), \forall T > 0$. These two points which seem open from the theoretical viewpoint are numerically observed. Consequently, we use in the sequel the following subset*

$$V_L = \{\omega \subset \Omega, |\omega| = L|\Omega|\}, \quad L \in (0,1) \tag{9}$$

where $|\omega|$ designates the measure of ω and replace (P_ω) by the problem $(P_{\omega,L}) : \inf_{\omega\in V_L} E(\omega, a, T)$ for L fixed in $(0,1)$. ■

It is well-known that the static version of (P_ω) - and *a fortiori* (P_ω) - is not well-posed on the set of admissible shapes V_L and has usually no solution ([9, 25]). In order to obtain existence of solutions, some geometrical constraints are required [18]. We mention for instance the perimeter constraint leading to a well-posed problem. Since the domain ω is assumed time-independent, it is easy to adapt results of the static case. Using the independence of the initial condition (y_0, y_1) with respect to ω and the decay of the energy, we obtain the following result (we refer to [21] for a study in the time-dependent case).

PROPOSITION 2.1 *Let $L \in (0,1)$. We assume that ω is of class $C^{1,1}(\Omega)$ (Uniformly lipschitz continuous on Ω). Then, there exists at least one $\omega \subset V_L$ minimizing the functional $\omega \to E(\omega, a, T)$.* ■

This work being devoted to numerical simulation, we do not reproduce the proof here and refer to [25] for a mathematical analysis. We also state without proof the following simpler result obtained using the independence of the initial condition with respect to the damping function a.

PROPOSITION 2.2 *Let $L \in (0,1)$. Let ω be fixed in V_L and $a(\boldsymbol{x}) = a\mathcal{X}_\omega(\boldsymbol{x})$. Then, there exists at least one scalar $a \in \mathbb{R}^+_\star$ minimizing the functional $a \to E(\omega, a, T)$.* ■

2.2 Shape derivative of the cost with respect to ω

From now, we simply denote $y_{\omega,a}$ by y. A standard procedure for this constrained problem $(P_{\omega,L})$ is to relax the condition $\omega \in V_L$ via a penalization parameter ε leading to the new problem:

$$(P^\varepsilon_{\omega,L}) : \inf_{\omega \subset \Omega} E^\varepsilon(\omega, a, T) \tag{10}$$

where

$$E^\varepsilon(\omega, a, T) = E(\omega, a, T) + \frac{1}{2}\varepsilon^{-1}(|\omega| - L\,|\Omega|)^2. \tag{11}$$

In order to solve $(P^\varepsilon_{\omega,L})$ using a gradient descent procedure, we now compute explicitly an expression of the derivative of the functional E^ε with respect to ω. The domain Ω is fixed and it is worth noticing that the initial condition (y_0, y_1) is independent of ω. Let $\eta \in \mathbb{R}^+$. From now on, we assume that ω is in $C^{1,1}(\Omega)$ and introduce a vector field $\boldsymbol{\theta} \in W^{1,\infty}(\Omega, \mathbb{R}^2)$, with $\boldsymbol{\theta}_{|\partial\Omega} = 0$ and $\boldsymbol{\theta}$ not vanishing on a neighborhood of $\partial\omega$.

DEFINITION 2.1 *The derivative of the functional E^ε with respect to a variation of $\omega \subset \Omega$ in the direction $\boldsymbol{\theta}$ is defined as the Fréchet derivative in $W^{1,\infty}(\Omega, \mathbb{R}^2)$ at 0 of the application $\boldsymbol{\theta} \to E^\varepsilon((Id + \eta\boldsymbol{\theta})(\omega))$, i.e.*

$$E^\varepsilon((Id + \eta\boldsymbol{\theta})(\omega), a, T) = E^\varepsilon(\omega, a, T) + \eta\frac{\partial E^\varepsilon(\omega, a, T)}{\partial \omega} \cdot \boldsymbol{\theta} + o(||\boldsymbol{\theta}||_{W^{1,\infty}(\Omega,\mathbb{R}^2)}). \tag{12}$$

■

We refer the reader to [9, 18] for more details. Moreover the derivative is a continuous linear form on $W^{1,\infty}(\Omega, \mathbb{R}^2)$ and depends only of the field $\boldsymbol{\theta}$ in an arbitrary small neighborhood of $\partial\omega$.

THEOREM 2.2 *The derivative of E^ε is given by the following expression:*

$$\frac{\partial E^\varepsilon(\omega, a, T)}{\partial \omega} \cdot \boldsymbol{\theta} = \int_{\partial\omega} \left[\varepsilon^{-1}(|\omega| - L|\Omega|) + a\int_0^T y'(\boldsymbol{x}, t)p(\boldsymbol{x}, t)dt\right]\boldsymbol{\theta} \cdot \boldsymbol{\nu} d\sigma \tag{13}$$

where $\boldsymbol{\nu}$ denotes the outward normal and p the solution of the following adjoint problem:

$$\left\{\begin{array}{lll} p'' - \Delta p - a(\boldsymbol{x})p' = 0 & in & \Omega \times (0,T), \\ p = 0 & on & (\partial\Omega \backslash \partial\omega) \times (0,T), \\ p(\boldsymbol{x},T) = -y'(\boldsymbol{x},T) & in & \Omega, \\ p'(\boldsymbol{x},T) = -a(\boldsymbol{x})y'(\boldsymbol{x},T) - \Delta y(\boldsymbol{x},T) & in & \Omega. \end{array}\right. \tag{14}$$

■

Remark 3 *If the function a takes the value a_1 on ω and a_2 on $\Omega\backslash\omega$, the derivative takes the form*

$$\frac{\partial E^{\varepsilon}(\omega,a,T)}{\partial\omega}\cdot\boldsymbol{\theta} = \int_{\partial\omega}\left[\varepsilon^{-1}(|\omega| - L|\Omega|) + \int_0^T [[a]]\, y'(\boldsymbol{x},t)p(\boldsymbol{x},t)dt\right]\boldsymbol{\theta}\cdot\boldsymbol{\nu}d\sigma \tag{15}$$

where the jump $[[a]]$ of a across $\partial\omega$ is defined as $[[a]] = a_1 - a_2$. In particular, if the jump is equal to zero and if $\omega \subset V_L$, then the derivative with respect to ω is null. ■

Remark 4 *From (3), $(p(T), p'(T)) \in (H_0^1(\Omega), L^2(\Omega))$. Therefore, the system (14) is well-posed and there exists a unique solution p such that*

$$p \in C((0,T); H_0^1(\Omega)) \cap C^1((0,T); L^2(\Omega)). \tag{16}$$

Consequently, $ay'p \in C((0,T); W^{1,1}(\Omega))$ and the derivative (13) is well-defined as a function on $\partial\omega$. ■

Proof of Theorem 2.2. In order to simplify the notations and to avoid duality products, we present a formal proof assuming the solution y and p are sufficiently regular to justify the integration by parts (we refer to [6] for rigorous developments). We associate with the system (1) a variational formulation keeping in mind that the domain Ω and ω are independent of time. For all $\varphi \in C((0,T); H_0^1(\Omega))$, we then consider the formulation

$$\left\{\begin{array}{l} \displaystyle\int_0^T\!\!\int_\Omega \Big(y''\varphi + \nabla y\cdot\nabla\varphi\Big)dxdt + \int_0^T\!\!\int_\omega ay'\varphi dxdt = 0, \\ \displaystyle\int_\Omega (y(.,0) - y_0)\varphi(.,0)\,dx = 0, \quad \int_\Omega (y'(.,0) - y_1)\varphi(.,0)\,dx = 0, \end{array}\right. \tag{17}$$

and apply the derivation method in order to obtain the formulation associated with the first lagrangian derivative Y. We obtain

$$\left\{\begin{array}{l} \displaystyle\int_0^T\!\!\int_\Omega (Y''\varphi + \nabla Y\cdot\nabla\varphi)dxdt + \int_0^T\!\!\int_\omega aY'\varphi dxdt \\ \qquad \displaystyle + \int_0^T\!\!\int_\Omega (\mathcal{A}(\boldsymbol{\theta})\cdot\nabla y\cdot\nabla\varphi + y''\mathrm{div}\boldsymbol{\theta}\varphi)dxdt + \int_0^T\!\!\int_\omega ay'\mathrm{div}\boldsymbol{\theta}\varphi dxdt = 0, \\ \displaystyle\int_\Omega (Y(.,0) - \nabla y_0\cdot\boldsymbol{\theta})\varphi(.,0)dx = 0; \quad \int_\Omega (Y'(.,0) - \nabla y_1\cdot\boldsymbol{\theta})\varphi(.,0)dx = 0. \end{array}\right. \tag{18}$$

The operator $\mathcal{A} : W^{1,\infty}(\Omega,\mathbb{R}^2) \to L^\infty(\Omega,\mathbb{R}^2)$ is defined as $\mathcal{A}(\boldsymbol{\theta}) = \mathrm{div}\boldsymbol{\theta} Id - (\nabla\boldsymbol{\theta} + \nabla\boldsymbol{\theta}^\star)$ where $\nabla\boldsymbol{\theta}^\star$ designates the transpose of $\nabla\boldsymbol{\theta}$. Using similar arguments, the derivative of the energy is

$$\begin{aligned} \frac{\partial E(\omega,a,T)}{\partial\omega}\cdot\boldsymbol{\theta} = \frac{1}{2}\int_\Omega \Big((|y'(T)|^2 + |\nabla y(T)|^2)\mathrm{div}\boldsymbol{\theta} - (\nabla\boldsymbol{\theta} + (\nabla\boldsymbol{\theta})^\star)\cdot\nabla y(T)\cdot\nabla y(T)\Big)dx \\ + \int_\Omega \Big(y'(T)Y'(T) + \nabla y(T)\cdot\nabla Y(T)\Big)dx. \end{aligned} \tag{19}$$

Let us rewrite this derivative in terms of y and p. A first computation leads to

$$\begin{aligned}\int_\Omega [y'(T)Y'(T) + \nabla y(T)\cdot\nabla Y(T)]dx = \\ \int_0^T\int_\Omega (p''Y - Y''p)dxdt + \int_\Omega (p'(0)Y(0) - p(0)Y'(0))dx + \int_\omega ay'(T)Y(T)dx.\end{aligned} \tag{20}$$

Using the formulation (1) and (14), we obtain that

$$\begin{aligned}\int_0^T\int_\Omega (p''Y - Y''p)dxdt = \int_\omega a(p(T)Y(T) - p(0)Y(0))dx \\ + \int_0^T\int_\Omega (\mathcal{A}(\boldsymbol{\theta})\cdot\nabla y\cdot\nabla p + y''p\,\mathrm{div}\boldsymbol{\theta})dxdt + \int_0^T\int_\omega ay'p\,\mathrm{div}\boldsymbol{\theta}dxdt.\end{aligned} \tag{21}$$

The relation $p(T) = -y'(T)$ then implies that

$$\begin{aligned}\frac{\partial E(\omega,a,T)}{\partial\omega}\cdot\boldsymbol{\theta} =& \frac{1}{2}\int_\Omega \Big((|y'(T)|^2 + |\nabla y(T)|^2)\mathrm{div}\boldsymbol{\theta} - (\nabla\boldsymbol{\theta} + (\nabla\boldsymbol{\theta})^\star)\cdot\nabla y(T)\cdot\nabla y(T)\Big)dx \\ &+ \int_0^T\int_\Omega (\mathcal{A}(\boldsymbol{\theta})\cdot\nabla y\cdot\nabla p + y''p\,\mathrm{div}\boldsymbol{\theta})dxdt + \int_0^T\int_\omega ay'p\,\mathrm{div}\boldsymbol{\theta}dxdt \\ &- \int_\omega ap(0)Y(0)dx + \int_\Omega (p'(0)Y(0) - p(0)Y'(0))dx.\end{aligned} \tag{22}$$

Then, from $\mathcal{A}(\boldsymbol{\theta})\cdot\nabla y\cdot\nabla p = (\theta_{1,1} - \theta_{2,2})(y_{,2}p_{,2} - y_{,1}p_{,1}) - (\theta_{1,2} + \theta_{2,1})(y_{,1}p_{,2} + y_{,2}p_{,1})$ and $\boldsymbol{\theta}_{|\partial\Omega} = 0$, we obtain

$$\begin{aligned}\int_0^T\int_\Omega (\mathcal{A}(\boldsymbol{\theta})\cdot\nabla y\cdot\nabla p + y''p\,\mathrm{div}\boldsymbol{\theta})dxdt &= \int_0^T\int_\Omega (\nabla p\cdot\boldsymbol{\theta}(\Delta y - y'') + \nabla y\cdot\boldsymbol{\theta}\Delta p - \nabla y''\cdot\boldsymbol{\theta}p)dxdt \\ &= \int_0^T\int_\omega \nabla p\cdot\boldsymbol{\theta}\,ay'dxdt + \int_0^T\int_\Omega (\nabla y\cdot\boldsymbol{\theta}\Delta p - \nabla y''\cdot\boldsymbol{\theta}p)dxdt.\end{aligned} \tag{23}$$

Additional integrations by part, using that $\boldsymbol{\theta}$ is time-independent, lead to the following expression

$$\begin{aligned}\frac{\partial E(\omega,a,T)}{\partial\omega}\cdot\boldsymbol{\theta} = \frac{1}{2}\int_\Omega \Big((|y'(T)|^2 + |\nabla y(T)|^2)\mathrm{div}\boldsymbol{\theta} - (\nabla\boldsymbol{\theta} + (\nabla\boldsymbol{\theta})^\star)\cdot\nabla y(T)\cdot\nabla y(T)\Big)dx \\ + \int_0^T\int_\omega \mathrm{div}(ay'p\,\boldsymbol{\theta})d\omega dt + \int_\Omega (\nabla y'(T)\cdot\boldsymbol{\theta}y'(T) - \nabla y(T).\boldsymbol{\theta}\Delta y(T))dx.\end{aligned} \tag{24}$$

Then, from $\mathrm{div}(|y'(T)|^2\boldsymbol{\theta}) = |y'(T)|^2\mathrm{div}\boldsymbol{\theta} + 2y'(T)\nabla y'(T).\boldsymbol{\theta}$ and the relation

$$\int_\Omega \nabla(|\nabla y(T)|^2)\cdot\boldsymbol{\theta}dx = -\int_\Omega (\nabla\boldsymbol{\theta} + \nabla\boldsymbol{\theta}^\star)\cdot\nabla y(T)\cdot\nabla y(T)dx - 2\int_\Omega \nabla y(T)\cdot\boldsymbol{\theta}\Delta y(T)dx \tag{25}$$

we finally obtain

$$\begin{aligned}\frac{\partial E(\omega,a,T)}{\partial\omega}\cdot\boldsymbol{\theta} =& \frac{1}{2}\int_\Omega \mathrm{div}((|y'(T)|^2 + |\nabla y(T)|^2)\boldsymbol{\theta})dx + \int_0^T\int_\omega \mathrm{div}(ay'p\boldsymbol{\theta})dxdt \\ &= \int_0^T\int_{\partial\omega} ay'p\,\boldsymbol{\theta}\cdot\boldsymbol{\nu}d\sigma dt\end{aligned} \tag{26}$$

using $\boldsymbol{\theta}_{|\partial\Omega} = 0$ in the first integral. Finally, from

$$\frac{\partial}{\partial\omega}(|\omega| - L\,|\Omega|)\cdot\boldsymbol{\theta} = \int_{\partial\omega}\boldsymbol{\theta}\cdot\boldsymbol{\nu}d\sigma. \tag{27}$$

we obtain the relation (13). ■

2.3 Derivative of the cost with respect to the coefficient a

We now assume that the domain ω is fixed in Ω and optimize E with respect to the value of the damping coefficient a. Since the cost is not monotonous with respect to a, it is not necessary to introduce a penalization argument here. Let us consider a perturbation of a:

$$a^\eta(\boldsymbol{x}) = a(\boldsymbol{x}) + \eta a^1(\boldsymbol{x}), \quad \boldsymbol{x} \in \Omega \tag{28}$$

assuming η small enough for a^η to remain in $L^\infty(\Omega, \mathbb{R}^+)$. We then assume that the variation of the solution of the wave equation can be written as follows: $y^\eta = y + \eta Y + O(\eta^2)$.

THEOREM 2.3 *The derivative of E with respect to a is*

$$\frac{\partial E(\omega, a, T)}{\partial a} \cdot a^1 = \int_0^T \int_\omega a^1 y'(\boldsymbol{x}, t) p(\boldsymbol{x}, t) dx dt \tag{29}$$

where p is solution of (14). ■

Proof. The proof is simpler than in the previous case. We obtain that Y and a^1 solve

$$\int_0^T \int_\Omega \Big(Y''\varphi + \nabla Y \cdot \nabla \varphi \Big) dx dt + \int_0^T \int_\omega (aY' + a^1 y')\varphi \, dx dt = 0, \quad \forall \varphi \in C((0,T); H_0^1(\Omega)). \tag{30}$$

Furthermore, since the initial conditions are independent of a, we have $Y(.,0) = 0$ and $Y'(.,0) = 0$ in Ω. The derivative of E with respect to a is then

$$\frac{\partial E^\varepsilon(\omega, a, T)}{\partial a} \cdot a^1 = \frac{\partial E(\omega, a, T)}{\partial a} \cdot a^1 = \int_\Omega \Big(y'(T)Y'(T) + \nabla y(T) \cdot \nabla Y(T) \Big) dx. \tag{31}$$

We then adapt (20) to obtain

$$\int_\Omega [y'(T)Y'(T) + \nabla y(T) \cdot \nabla Y(T)] dx = \int_0^T \int_\Omega (p''Y - Y''p) dx dt + \int_\omega a y'(T) Y(T) dx. \tag{32}$$

Y being solution of (30), we obtain

$$\begin{aligned} \int_0^T \int_\Omega (p''Y - Y''p) dx dt &= \int_\omega a(Y(T)p(T) - Y(0)p(0)) dx + \int_0^T \int_\omega a^1 y' p \, dx dt \\ &= -\int_\omega a Y(T) y'(T) dx + \int_0^T \int_\omega a^1 y' p \, dx dt \end{aligned} \tag{33}$$

and finally the relation (29). ■

2.4 Topological derivative

In a similar manner, we may also compute the topological derivative associated with E, notion introduced in [28] and then used efficiently in the context of shape optimization (see for instance [2, 13]).

THEOREM 2.4 *For any $\boldsymbol{x_0} \in \Omega$ and ρ such that $D(x_0, \rho) \equiv \{\boldsymbol{x} \in \mathbb{R}^2, dist(\boldsymbol{x}, \boldsymbol{x_0}) \leq \rho\} \subset \Omega$, the functional associated with $D(\boldsymbol{x_0}, \rho)$ may be expressed as follows:*

$$E(D(\boldsymbol{x_0}, \rho), a, T) = E(\emptyset, a, T) + \pi\rho^2 \int_0^T a y'_{\emptyset,0}(\boldsymbol{x_0}, t) p_{\emptyset,0}(\boldsymbol{x_0}, t) dt + o(\rho^2) \tag{34}$$

in terms only of the conservative solutions $y_{\emptyset,0}, p_{\emptyset,0}$. The term factor of ρ^2 is called the topological derivative of E. ■

Proof. The computation is very similar to the computation of the shape derivative (we refer the reader to [28] for general developments). In our simple situation, we may obtained a relation similar to (34) by using the interplay between ω and a (i.e. $E(\omega,0,T)=E(\emptyset,a,T)$ for all a and ω) and the variation of E with respect to a. Precisely, taking $a=0$ and $\omega=D(\boldsymbol{x_0},\rho)\subset\Omega$ in the equality

$$E(\omega,a+\eta a^1,T)=E(\omega,a,T)+\eta a^1\int_\omega\int_0^T y'_{\omega,a}(\boldsymbol{x},t)p_{\omega,a}(\boldsymbol{x},t)dtdx+o(\eta) \tag{35}$$

leads to

$$E(D(\boldsymbol{x_0},\rho),\eta a^1,T)=E(D(\boldsymbol{x_0},\rho),0,T)+\eta a^1\int_{D(\boldsymbol{x_0},\rho)}\int_0^T y'_{\emptyset,0}(\boldsymbol{x},t)p_{\emptyset,0}(\boldsymbol{x},t)dtdx+o(\eta). \tag{36}$$

and then from $E(D(\boldsymbol{x_0},\rho),0,T)=E(\emptyset,\eta a^1,T)$ (and replacing ηa^1 by a), we obtain the difference of the energies associated with the dissipative and conservative case respectively, in function only of the solution of the conservative case $y_{\emptyset,0}$ and $p_{\emptyset,0}$

$$E(D(\boldsymbol{x_0},\rho),a,T)=E(\emptyset,a,T)+a\int_{D(\boldsymbol{x_0},\rho)}\int_0^T y'_{\emptyset,0}(\boldsymbol{x},t)p_{\emptyset,0}(\boldsymbol{x},t)dtdx+o(a). \tag{37}$$

We then easily get (34). Once again, these relation highlights the balance between a and ω (or equivalently ρ) and will illustrates the over-damping phenomenon. We will use these relation to obtain an efficient prediction of ω, for a or ρ small enough (see Section 5). □

3 Minimization of the cost

Thanks to the previous computations, we are now in position to apply a gradient descent method for the minimization of the objective function E^ε with respect to the position of ω and for E with respect to the value of the function a respectively.

3.1 Minimization of E^ε with respect to ω - Level set approach

From (13), the shape derivative is

$$\frac{\partial E^\varepsilon(\omega,a,T)}{\partial\omega}\cdot\boldsymbol{\theta}=\int_{\partial\omega}j^\varepsilon(y_{\omega,a},p_{\omega,a},T)\boldsymbol{\theta}\cdot\boldsymbol{\nu}\,d\sigma \tag{38}$$

with $j^\varepsilon(y_{\omega,a},p_{\omega,a},T)=\varepsilon^{-1}(|\omega|-L|\Omega|)+a\int_0^T y'_{\omega,a}(\boldsymbol{x},t)p_{\omega,a}(\boldsymbol{x},t)dt$ defined on Ω. A descent direction is found by defining on $\partial\omega$ the vector field $\boldsymbol{\theta}$ as follows :

$$\boldsymbol{\theta}=-j^\varepsilon(y_\omega,p_\omega,T)\boldsymbol{\nu}, \tag{39}$$

and we then update the shape ω as $\omega^\eta=(Id+\eta\boldsymbol{\theta})(\omega)$ (we recall that ω is in $C^{1,1}(\Omega)$). The parameter $\eta>0$ denotes a descent step small enough so that the formal following relation

$$E^\varepsilon(\omega^\eta,a,T)=E^\varepsilon(\omega,a,T)-\eta\int_{\partial\omega}(j^\varepsilon(y_{\omega,a},p_{\omega,a},T))^2d\sigma+O(\eta^2) \tag{40}$$

guarantees the decrease of E^ε. This method can be implemented in the Lagrangian framework : it suffices to mesh the domains ω, $\Omega\backslash\omega$ and then advect the mesh according to the descent direction $\boldsymbol{\theta}$ defined on $\partial\omega$ by (39). This imposes to mesh the moving interface $\partial\omega$. Morever, the re-meshing of the domain at each step may produce a costly method. Finally, the change of topology of $\partial\omega$ is quite difficult to handle with this approach. Therefore,

following recent works in optimal shape design [1, 31], we adopt an Eulerian approach and we use a level-set method to capture the shape ω on a fixed mesh. Let us briefly recall the main features of this method. The level set approach introduced in [27] (see [29, 30] for a survey) consists in giving a description of the evolving interface $\partial\omega$ independent of the discretizing mesh on Ω. We define the level-set function ψ in Ω in such a way that

$$\psi(\boldsymbol{x}) \leq 0 \quad \boldsymbol{x} \in \omega, \quad \psi(\boldsymbol{x}) = 0 \quad \boldsymbol{x} \in \partial\omega, \quad \psi(\boldsymbol{x}) \geq 0 \quad \boldsymbol{x} \in \Omega\backslash\omega. \tag{41}$$

Therefore, the evolving interface $\partial\omega$, is characterized by

$$\partial\omega = \{\boldsymbol{x}(\tau) \in \Omega \text{ such that } \psi(\boldsymbol{x}(\tau), \tau) = 0\}, \tag{42}$$

where τ denotes a pseudo-time variable, increasing with time, that may be the real time, a load factor or in our case, the iterations of a given algorithm. Differentiation of (42) with respect to τ then leads to

$$\frac{\partial\psi}{\partial\tau}(\boldsymbol{x}(\tau), \tau) + \nabla\psi(\boldsymbol{x}(\tau), \tau) \cdot \frac{d\boldsymbol{x}(\tau)}{d\tau} = 0. \tag{43}$$

Denoting by $\boldsymbol{F}$ the speed in the outward normal direction, such that $\frac{d\boldsymbol{x}(\tau)}{d\tau} \cdot \boldsymbol{\nu} = \boldsymbol{F}(\boldsymbol{x}(\tau))$ where $\boldsymbol{\nu} = \nabla\psi/|\nabla\psi|$, we obtain the following nonlinear Hamilton-Jacobi equation of the first order for ψ:

$$\frac{\partial\psi}{\partial\tau}(\boldsymbol{x}, \tau) + F(\boldsymbol{x}, \tau)|\nabla\psi(\boldsymbol{x}, \tau)| = 0, \quad \text{given} \quad \psi(\boldsymbol{x}, \tau = 0). \tag{44}$$

Assuming that the shape $\partial\omega$ evolves in pseudo-time τ with the normal velocity $\boldsymbol{F} = -j^\varepsilon(y_{\omega,a}, p_{\omega,a}, T)\boldsymbol{\nu}$ as proposed in (39), the transport of the level set function ψ is therefore equivalent to moving the boundary of ω (the zero level-set of ψ) along the descent gradient direction $-\partial E^\varepsilon/\partial\omega$. Consequently, the partial differential system which has to be solved is given by

$$\begin{cases} \dfrac{\partial\psi}{\partial\tau} - j^\varepsilon(y_{\omega,a}, p_{\omega,a}, T)|\nabla\psi| = 0 \quad \text{in} \quad \Omega \times (0, \infty), \\ \psi(., \tau = 0) = \psi_0 \quad \text{in} \quad \Omega, \\ \psi = \psi_0 > 0 \quad \text{on} \quad \partial\Omega \times (0, \infty). \end{cases} \tag{45}$$

We further impose that ψ be constant and positive on Ω in order to ensure that $\partial\omega \cap \partial\Omega = \emptyset$. Finally, because of its advection, the level-set function may becomes too flat or too steep yielding either large errors in the location of its zero level or large errors in the evaluation of its gradient by finite differences. Therefore, a standard trick (see [30]) consists in replacing the level-set ψ at the pseudo time τ_0 by the regularized one, which solves the following problem

$$\begin{cases} \dfrac{\partial\tilde{\psi}}{\partial\tau} + \text{sign}(\psi(\tau_0))(|\nabla\tilde{\psi}| - 1) = 0 \quad \text{in} \quad \Omega \times (0, \infty), \\ \tilde{\psi}(., \tau = 0) = \psi(\tau_0) \quad \text{in} \quad \Omega, \end{cases} \tag{46}$$

admitting as a stationary solution the signed distance to the initial interface $\{\psi(\boldsymbol{x}, \tau_0) = 0\}$.

3.2 Minimization of E with respect to a

Similarly, we use the expression (29) to minimize the cost function with respect to a. a being constant on ω, a descent direction is obtained by defining a^1 as follows :

$$a^1 = -\int_0^T \int_\omega y'(\boldsymbol{x}, t)p(\boldsymbol{x}, t)dxdt. \tag{47}$$

Then, we update a on ω as $a^\eta = a + \eta a^1$ on ω where $\eta > 0$ designates a descent step small enough so that

$$E(\omega, a^\eta, T) = E(\omega, a, T) - \eta\left(\int_0^T \int_\omega y'(\boldsymbol{x}, t)p(\boldsymbol{x}, t)dxdt\right)^2 + O(\eta^2) \tag{48}$$

guarantees the decrease of E.

Remark 5 *If we assume that a may vary in ω, then the descent direction is*

$$a^1(\boldsymbol{x}) = -\int_0^T y'(\boldsymbol{x}, t)p(\boldsymbol{x}, t)\, dt \tag{49}$$

leading to

$$\frac{\partial E(\omega, a, T)}{\partial a} \cdot a^1 = -\int_\omega \left(\int_0^T y'(\boldsymbol{x}, t)p(\boldsymbol{x}, t)dt\right)^2 dx. \tag{50}$$

■

4 Numerical Approximation - Optimization Algorithm

We present in this section some important numerical aspects. In particular, we focus on the importance of adding some *viscosity* terms in the usual discrete approximation of the wave systems (1) and (14), more sensitive to the numerical approximation than elliptic or parabolic systems.

4.1 Resolution of the wave equations (1) and (14) - Introduction of viscosity terms

For simplicity, we take $\Omega = (0, 1)^2$ and choose to approximate the wave system with finite difference schemes. Let us consider $J \in \mathbb{N}$, $h = 1/(J + 1)$ and a uniform grid $(x_{1,i}, x_{2,j})_{(i,j)}$ of Ω such that $0 = x_{k,0} < x_{k,1} < ... < x_{k,J} < x_{k,J+1} = 1$, with $x_{k,j} = jh$ and $k = 1, 2$. Let us also consider $N \in \mathbb{N}$, $\Delta t = T/N$ and a uniform grid of the time interval $(0, T)$ given by $0 = t_0 < t_1 < ... < t_N = T$, with $t_n = n\Delta t$. h and Δt denotes the space and time step respectively. Let us denote by $y^n_{i,j}$ the approximation of y at the point $(x_{1,i}, x_{2,j})$ and time t_n:

$$y^n_{i,j} \approx y(x_{1,i}, x_{2,j}, t_n), \quad 0 \le i, j \le J + 1, \quad 0 \le n \le N. \tag{51}$$

The simplest way (see [8]) to approximate the wave equation is to approximate the derivative in time by a centered finite difference as follows :

$$2\Delta t\, y' = y^{n+1} - y^{n-1} + O(\Delta t^3), \quad \Delta t^2\, y'' = y^{n+1} - 2y^n + y^{n-1} + O(\Delta t^4), \tag{52}$$

and to approximate the Laplacian by the 5 points finite difference

$$h^2\Delta y(x_{1,i}, x_{2,j}) = y_{i+1,j} + y_{i-1,j} + y_{i,j+1} + y_{i,j-1} - 4y_{i,j} + O(h^4) \equiv h^2\Delta_h y_{i,j} + O(h^4) \tag{53}$$

leading to a centered scheme of order two in space and time, and stable under the condition $\Delta t \le h/\sqrt{2}$ (we refer to [24] for the details). However, as observed initially in [3] in the context of stabilization and in [14] in the context of exact controllability, this scheme is not uniformly convergent with respect to the dissipation property. The interaction of waves with a numerical mesh produces dispersion phenomena and spurious high frequencies. Because of this nonphysical interaction of waves with the discrete medium, the velocity of propagation of numerical waves may converge to zero when the wavelength of solutions is of the order of the size of the mesh. Consequently, the time needed to uniformly damp the numerical waves

from a subset of $\Omega\backslash\omega$ in which they propagate may tend to infinity as the mesh becomes finer. Thus, the dissipation mechanism may disappear completely if the initial conditions are represented by high frequency components (see [24] for numerical illustrations). This is the case for discontinuous initial data. Mathematically speaking, the convergence of the solution in the energy norm is not ensured. We replace the standard scheme by the scheme associated with the following equation

$$y'' - \Delta y + a(\boldsymbol{x})y' - h^2\Delta y' = 0 \quad \text{in} \quad \Omega \times (0,T) \tag{54}$$

including a so-called viscous term $h^2\Delta y'$ negligible for the low frequency components and of order of the energy for the high frequency ones. The modified implicit scheme is then :

$$\begin{cases} \left(1 + \dfrac{\Delta t}{2}(a_{i,j} - \Delta_h)\right) y_{i,j}^{n+1} = (2 + r^2\Delta_h) y_{i,j}^n - \left(1 - \dfrac{\Delta t}{2}(a_{i,j} - \Delta_h)\right) y_{i,j}^{n-1}, \\ \qquad\qquad 1 \le i,j \le J, \quad 1 \le n \le N, \\ y_{i,j}^n = 0, \quad i = \{0, J+1\} \quad \text{or} \quad j = \{0, J+1\}, \quad 1 \le n \le N, \\ y_{i,j}^0 = y_0(x_{1,i}, x_{2,j}), \quad y_{i,j}^1 = (1 + \dfrac{r^2}{2}\Delta_h) y_{i,j}^0 + \Delta t\, y_1(x_{1,i}, x_{2,j}), \quad 1 \le i,j \le J, \end{cases} \tag{55}$$

where $r = \Delta t/h$. It is shown in [24] that this scheme is a convergent approximation of (1) under the condition $\Delta t \le h/\sqrt{2}$ and provides a uniform approximation of the energy as h and Δt go to zero. The same modification is needed for the adjoint problem. This is due to the fact that the initial conditions at time T defined by $p(T) = -y'(T)$ and $p'(T) = a(\boldsymbol{x})p(T) - \Delta y(T)$ are *a priori* less regular than y_0 and y_1. Therefore, we consider the discretization of the following equation

$$p'' - \Delta p - a(\boldsymbol{x})p' + h^2\Delta p' = 0 \quad \text{in} \quad \Omega \times (0,T) \tag{56}$$

leading to :

$$\begin{cases} \left(1 + \dfrac{\Delta t}{2}(a_{i,j} - \Delta_h)\right) p_{i,j}^{n-1} = (2 + r^2\Delta_h) p_{i,j}^n - \left(1 - \dfrac{\Delta t}{2}(a_{i,j} - \Delta_h)\right) p_{i,j}^{n+1}, \\ \qquad\qquad 1 \le i,j \le J, \quad 1 \le n \le N \\ p_{i,j}^n = 0, \quad i = \{0, J+1\} \quad \text{or} \quad j = \{0, J+1\}, \quad 1 \le n \le N \\ p_{i,j}^N = -\dfrac{y_{i,j}^{N+1} - y_{i,j}^{N-1}}{2\Delta t}, \quad p_{i,j}^{N-1} = (1 - a_{i,j}\Delta t) p_{i,j}^N + \dfrac{\Delta t}{h^2}\Delta_h y_{i,j}^N, \quad 1 \le i,j \le J. \end{cases} \tag{57}$$

4.2 Resolution of the Hamilton-Jacobi equation

Let us now consider the resolution of the non-linear Hamilton-Jacobi equation (45). We introduce a parameter $\Delta\tau > 0$ and note by $\psi_{i,j}^k$ the approximation of the function ψ at the point $x_{i,j} = (x_{1,i}, x_{2,j})$ and at the pseudo-time $\tau = k\Delta t$. We note by $j_{i,j}^\varepsilon$ the approximation of $j^\varepsilon(y_{\omega,a}(x_{i,j}), p_{\omega,a}(x_{i,j}))$ such that

$$j_{i,j}^\varepsilon = \varepsilon^{-1}(|\omega_h| - L|\Omega_h|) + a_{i,j} \sum_{n=0}^{N} \frac{y_{i,j}^{n+1} - y_{i,j}^{n-1}}{2} p_{i,j}^n \tag{58}$$

where $a_{i,j} = a(x_{i,j}) = a\mathcal{X}_{(\psi_{i,j} \le 0)}$, $|\Omega_h| = 1$ and $|\omega_h| = \|\mathcal{X}_{(\psi_h(x_{i,j}) \le 0)}\|_{L_h^1(\Omega)}$. The hyperbolic system (45) is solved using an explicit weighted essentially non-oscillatory scheme of order one in pseudo-time τ and of order two in space (see [29, 30] for a complete description):

$$\frac{\psi^{k+1} - \psi^k}{\Delta\tau} + \left(\max(-j^\varepsilon(y^k, p^k), 0)\nabla_k^+ + \min(-j^\varepsilon(y^k, p^k), 0)\nabla_k^-\right) = 0, \quad k > 0 \tag{59}$$

where (∇_k^+, ∇_k^-) designates forward and upward approximation of $|\nabla\psi^k|$. This explicit scheme is stable under the condition $\Delta\tau \leq h/\max_\Omega|j^\varepsilon(y^k,p^k)|$. Finally, in order that the pseudo-time step $\Delta\tau$ decreases with respect to the iteration k, we consider the following pseudo-time step

$$\Delta\tau^k = \min\Big(1, \max_\Omega|j^\varepsilon(y^k,p^k)|\Big)\frac{h}{\max_\Omega|j^\varepsilon(y^k,p^k)|} \quad (\leq \Delta\tau^{k-1}), \quad \forall k>0. \tag{60}$$

Remark 6 *The upwind scheme (59) is motivated by the propagation of information through characteristics in the first order hyperbolic equation (44). Very interestingly with respect to the discussion of the previous section, this scheme may be replaced by usual centered finite differences ones, provided the addition of an artificial viscosity term (see [29]) (namely the approximation of $\psi_\tau + F|\nabla\psi| = h\Delta\psi$ instead of (44)). The reason to introduce this term here is however different.* ■

4.3 Optimization algorithm

The algorithm to solve numerically the problem $(P^\varepsilon_{\omega,L})$ may be structured as follows :

(i) Meshing once for all of the fixed domain Ω. Initialization of the level-set ψ_0 corresponding to an initial guess ω_0 (obtained for instance using (34) or (37))

(ii) Iteration until convergence, for $k \geq 0$:

- Computation on Ω of the state y^k, solution of the forward wave system (1) using the scheme (55).
- Computation of the adjoint state p^k, solution of the backward wave system (14) using the scheme (57).
- Computation on Ω of the integrand $j^\varepsilon(y^k,p^k)$ (see Theorem 2.2) using the approximation (58).
- Deformation of the shape by solving the transport Hamilton-Jacobi system (45) using the scheme (59). The new domain ω_{k+1} is characterized by the level-set function ψ^{k+1} solution of (45) after a pseudo-time step $\Delta\tau^k$ starting from the initial condition ψ^k with velocity $-j^\varepsilon(y^k,p^k)$. The pseudo-time step $\Delta\tau^k$ is chosen according to (60). The value $\Delta\tau^k$ monitored by the stability condition (60) is usually small enough to ensure the decrease of the cost function.

(iii) From time to time, for stability reasons, we re-initialize the level-set function ψ by solving (46) using a scheme analogous to (59) .

Since, for each iteration, the computation of the state y^k and the adjoint p^k is much more expensive in CPU time than the resolution of the Hamilton-Jacobi system, we perform several explicit pseudo-time steps of (45) after each resolution of (1) and (14). During these explicit pseudo-time steps, we perform regularly some re-initialization of the level set function by solving (46).

Remark 7 *One of the main advantage of the level-set method is to easily handle topology changes, i.e. merging and cancellations of holes. Under the strict stability condition (60), the algorithm can not create holes. This is a consequence of the maximum principle associated to the solution of (45). Therefore, the only possible mechanism is that an initial hole splits in two new holes. This phenomenon will appear in one example developed in Section 5.* ■

The algorithm used to solve problem (P_a) has a similar structure. The integrand is obtained by approximating (47) or (49).

Finally, we will consider in the application the optimization of the energy with respect to ω and a simultaneously, i.e.

$$\inf_{\omega\in V_L,\, a\in L^\infty(\Omega,\mathbb{R}^+)} E^\varepsilon(\omega,a,T). \tag{61}$$

An iteration of the gradient algorithm may be then written as follows :

$$\begin{pmatrix} \omega_{k+1} \\ a_{k+1} \end{pmatrix} = \begin{pmatrix} \omega_k \\ a_k \end{pmatrix} - \begin{pmatrix} \eta_1 \boldsymbol{\nu}_k \\ \eta_2 \end{pmatrix} . \begin{pmatrix} \varepsilon^{-1}(|\omega_k| - L|\Omega|) + \int_0^T a_k y_k' p_k dt \\ \int_0^T \int_{\omega_k} y_k' p_k dx dt \end{pmatrix} \tag{62}$$

with $\eta = (\eta_1, \eta_2)$ small enough.

5 Numerical experiments

We now present some numerical simulations. In all the computations, the domain Ω is the unit square. A uniform mesh is used with $h = 1/150$ and $\Delta t = h/\sqrt{2}$. We first consider smooth initial conditions, and then some irregular ones in order to stress the necessity of the additional viscosity term in the discretization of the wave system.

5.1 Regular initial conditions

5.1.1 Minimization with respect to ω

We assume that the function a is fixed. We first consider the following regular initial condition function of the first frequency component:

$$y_0(\boldsymbol{x}) = 100\sin(\pi x_1)\sin(\pi x_2), \quad y_1(\boldsymbol{x}) = 0., \quad \boldsymbol{x} = (x_1, x_2) \in \Omega. \tag{63}$$

We take $L = 1/10$, $\varepsilon = 10^{-5}$, $T = 1$ and $a(\boldsymbol{x}) = 10\,\mathcal{X}_\omega(\boldsymbol{x})$. Before giving numerical results, let us apply the relation (37). Let $\alpha = \sqrt{2}\pi$. The conservative solution associated with (y_0, y_1) is $y_{\omega,0}(\boldsymbol{x}, t) = \cos(\alpha t) y_0(\boldsymbol{x})$ so that

$$\begin{cases} p_{\omega,0}(\boldsymbol{x},t) = \alpha\sin(\alpha T) y_0(\boldsymbol{x}), \quad p'_{\omega,0}(\boldsymbol{x},t) = \alpha^2\cos(\alpha T) y_0(\boldsymbol{x}), \\ p_{\omega,0}(\boldsymbol{x},t) = \alpha\Big(\sin(\alpha T)\cos(\alpha(t-T)) + \cos(\alpha T)\sin(\alpha(t-T))\Big) y_0(\boldsymbol{x}) \end{cases} \tag{64}$$

and $\int_0^T y'(\boldsymbol{x},t)p(\boldsymbol{x},t)dt = -\frac{\alpha}{4}(2\alpha T - \sin(2\alpha T))y_0(\boldsymbol{x})^2 < 0$. From the relation (37), we have

$$E(\omega,a,T) - E(\omega,0,T) = -\frac{a\alpha}{4}(2\alpha T - \sin(2\alpha T))\int_\omega (y_0(\boldsymbol{x}))^2 dx + o(a),\ \forall T \geq 0. \tag{65}$$

For a small enough and for all $T > 0$, the dissipation is then optimal for ω which maximizes the integral $\int_\omega (y_0(\boldsymbol{x}))^2 dx$, i.e. centered on the unit square Ω. The simulations confirm this prediction. Figure 2 depicts the evolution of the zero-level set $\{\boldsymbol{x} \in \Omega, \psi_k(\boldsymbol{x}) = 0\} = \partial\omega_k$ with respect to the iteration k (equivalently with respect to the pseudo-time parameter $\tau > 0$). Let us denote by $\omega_{(c)}$ the disc of radius $\sqrt{L/\pi}$ and center (c, c). The sequence of domain ω_k is initialized by $\omega_0 = \omega_{(0.35)}$ so that $|\omega_0| = L$ (the boundary $\partial\omega_0$ is in dash-dot on Figure 2). Figure 3 depicts the cost function and $|\omega_k|$ with respect to k. As expected, the limit of the sequence $(\omega_k)_{k>0}$ is near from a disc centered on $(1/2, 1/2)$. We check that we obtain exactly a disc when Ω is itself a disc. We also observe that the value of $\varepsilon = 10^{-5}$ is small enough to maintain $|\omega_k|$ near from L. This result is invariant with respect to T and also with respect to the initialization ω_0. Figures 4 and 5 display the evolution of $\partial\omega_k$ when ω_0 is composed of 4 and 9 disjoints discs respectively. Figures 6 and 7 and

display the evolution of the corresponding area and cost. The limit cost functions obtained with these three initializations are very similar. Let us now consider the initial condition $y_0(\boldsymbol{x}) = 100\sin(2\pi x_1)\sin(\pi x_2)$ for which $y_{\omega,0}(\boldsymbol{x},t) = 100\cos(\sqrt{5}\pi t)\sin(2\pi x_1)\sin(\pi x_2)$. The relation (65) still holds for $\alpha = \sqrt{5}\pi$ showing that for a small enough, the optimal position of ω is related to the points $(1/4, 1/2)$ and $(3/4, 1/2)$ where the function y_0^2 admits two maxima. Once again, the numerical simulations are in good agreement with this prediction. Figures 8 and 9 display the evolution of the sequence $(\omega_k)_{k>0}$ when ω_0 is composed of one and one hundred disjoints parts respectively. For these examples, the invariance with respect to ω_0 illustrates (for a small) the uniqueness of the minimum.

On the other hand, with more general initial condition (for instance without symmetries in space), the limit of the sequence $(\omega_k)_{k>0}$ may depend on both ω_0 and T, highlighting the presence of local minima. In this case, we observe that an initialization ω_0 composed of several components provides a lower value of the cost (i.e. a better local minima). Figure 10 displays the limit of $\partial\omega_k$ for $T = 1$ and $T = 2$ and four configurations of ω_0 when $y_0(\boldsymbol{x}) = 300x_1x_2(x_1-1)(x_2-1)\cos(5\pi x_1(x_2-1))\sin(2\pi x_1x_2)$ and $y_1 = 0$. Table 10 gives the energy $E(\omega, a, T)$ associated with these limits. Remark that the existence of several local minima does not imply necessarily that the problem (P_ω) is ill-posed: since a finite number of frequency component is present in y_0 and since a is small, we may conjecture that the optimal design is composed by a finite number of disjoint components. For these data, Figure 11 depicts the topological derivative $\boldsymbol{x} \to \int_0^T y'_{\emptyset,0}(\boldsymbol{x},t)p_{\emptyset,0}(\boldsymbol{x},t)dt$ in Ω (see eq. 37); the corresponding characteristic function (on the bottom) of size L illustrates how this derivative provides an efficient initialization (we refer to [2, 13] for a strong coupling between level set and topological derivative).

T	$\sharp\,\omega_0 = 1$	$\sharp\,\omega_0 = 9$	$\sharp\,\omega_0 = 25$	$\sharp\,\omega_0 = 49$
1	502.64	261.88	256.86	249.10
2	322.88	117.99	96.53	88.17

Table 1: $E(\omega, a = 10., T)$ for different initial predictions ω_0 - $\sharp\,\omega_0$: number of disjoint parts of ω_0 - (associated with Fig. 10).

5.1.2 Minimization with respect to the damping function a

We consider once again the initial condition $y_0(\boldsymbol{x}) = 100\sin(\pi x_1)\sin(\pi x_2)$, $y_1 = 0$, fixe ω and optimize with respect to a. Figure 12 represents the energy $E(\omega_{(1/2)}, a, 1)$ with respect to the constant a on $\omega = \omega_{(1/2)}$. The minimum of the energy with respect to a is obtained for $a \approx 15.33$ and $E(\omega_{(1/2)}, 15.33, 1) \approx 439.59$. The value 15.33 is obtained using the descent direction (47). Figure 12 illustrates the over-damping phenomenon : since $y_1 = 0$, $E(\omega, a, T = 1)$ converges towards $E(\omega, a, 0) = E(\emptyset, 0, 0) = E(\omega, 0, T)$ as a goes to infinity. Numerically, we obtain $E(\omega, 0, T) - E(\omega, a, T) \approx O(a^{-0.78})$.

Obviously, the value 439.59 is improved if we assume that the function a may depends on $\boldsymbol{x}$ in ω. Figure 13 describes the graph of $a_k(x_1, 1/2), x_1 \in [0, 1]$ for different iterations k of the descent algorithm using the direction (49). We observe, in agreement with the theoretical analysis in [12, 20], that the functions $a_k(\boldsymbol{x})$ take negative values in ω. We also observe that the norm $\|a_k\|_{L^\infty(\omega)}$ is not bounded with respect to k: precisely, on the boundary of ω, the function a_k tends to infinity with k. This simulation suggests that the derivative of the damping potential is as important as his sign for the dissipation. This is in agreement with [7] where it is shown that the unbounded function $a(x) = 1/x$ in $(0, 1)$ extinguishes in finite time the solution of the 1-d damped wave equation. We remark however that the average $\int_\omega a_k(\boldsymbol{x})dx/|\omega|$ remains bounded and converges as k goes to infinity to the value 15.33 (optimal for a constant in ω). These observations illustrate the influence of the over-damping phenomenon and the richness of problem (P_a). The optimal value of a

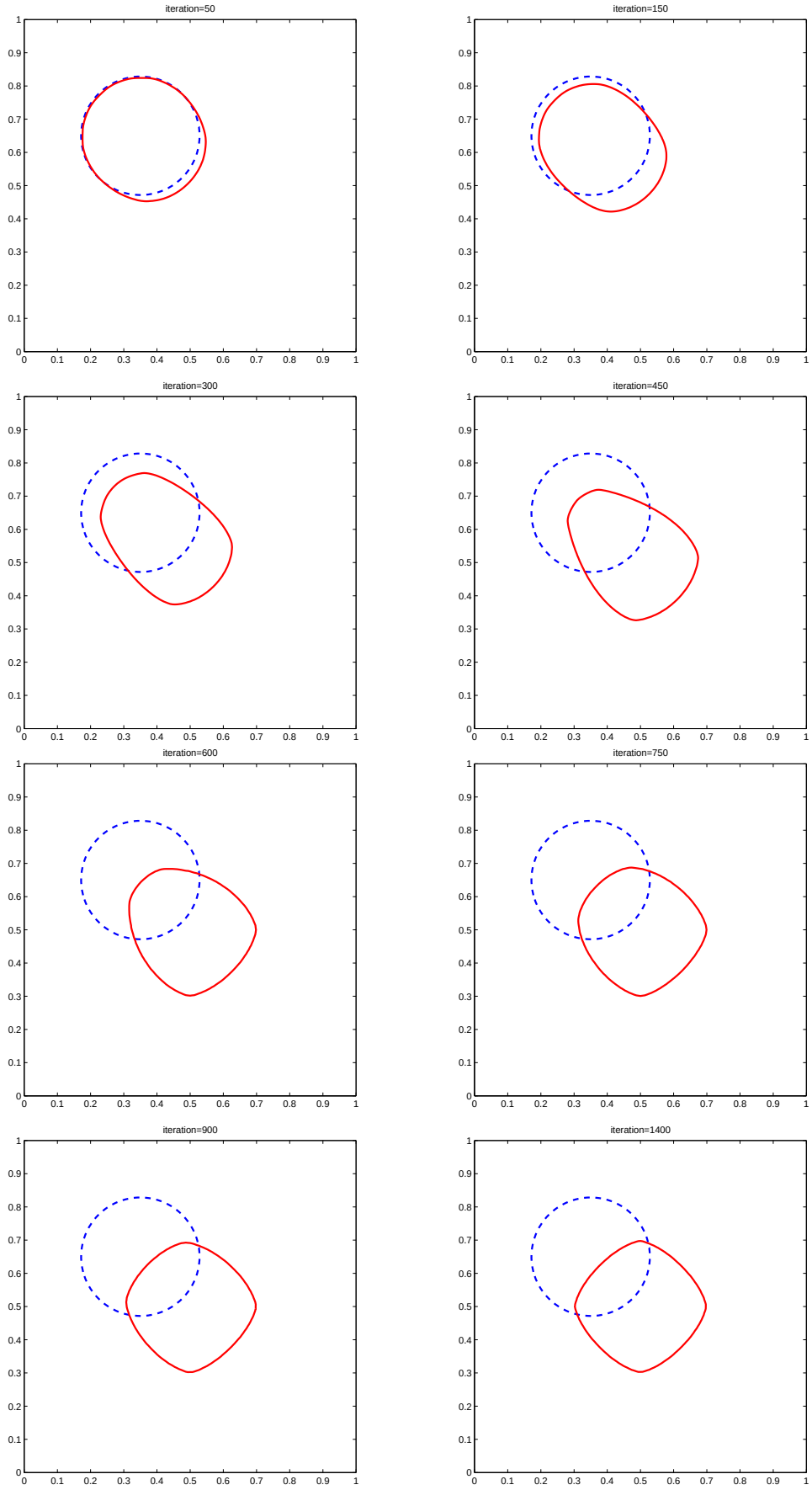

Figure 2: $(y_0, y_1) = (100\sin(\pi x_1)\sin(\pi x_2), 0)$, $T = 1.$, $a = 10.$ - Evolution of the zero-level set $\{\boldsymbol{x} \in \Omega, \psi_k(\boldsymbol{x}) = 0\}$ with respect to k.

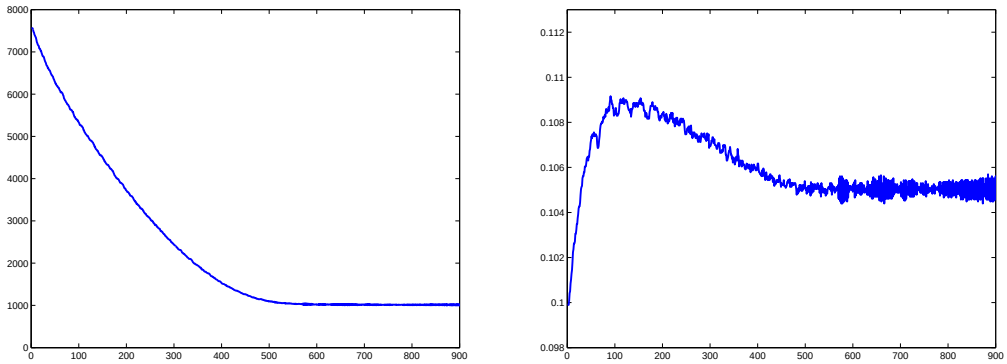

Figure 3: $(y_0, y_1) = (100\sin(\pi x_1)\sin(\pi x_2), 0)$, $T = 1$ - Evolution of $E(\omega_k, a, T)$ (**Left**) and $|\omega_k|$) (**Right**) with respect to k (associated with Fig. 2).

depends also on the domain ω. For instance, for $\omega = \omega_{(0.35)}$, the optimal damping constant is $a \approx 24.89$ leading to $E(\omega_{(0.35)}, 24.89, 1) \approx 4916.93$.

Very interestingly, if we now come back to the problem (P_ω) with a larger value than $a = 10.$ (used in Section 5.1.1) - for instance $a = 25$ - and $\omega_0 = \omega_{(0.35)}$, we do not obtain anymore a centered disc. The limit in k of the zero-level set $\{\boldsymbol{x} \in \Omega, \psi_k(\boldsymbol{x}) = 0\}$ is depicted on Figure 14 (top left) leading to a cost $E(\omega_{(0.35)}, a = 25, T) \approx 101.08$ (in comparison with $E(\omega_{(1/2)}, 15.33, T) \approx 439.59 < E(\omega_{(1/2)}, a = 25, T)$). At the limit, the domain ω is divided in three parts ! Remark that this point is not in contradiction with the relation (65) because the value $a = 25$ is not "small" enough. We remark that this value is on the increasing part of the function $a \to E(\omega, a, T)$ (see Figure 12) whereas the value $a = 10.$ used in Section 5.1.1 is on the decreasing part. Moreover, for this value, the invariance with respect to the initialization ω_0 is lost. Figure 14 depicts the limit in k of the zero-level set $\{\boldsymbol{x} \in \Omega, \psi_k(\boldsymbol{x}) = 0\}$ for three other initial predictions ω_0. Even for a symmetric ω_0 (Fig. 14 bottom right), the limit is not a centered disc but is associated with a limit cost function $E(\omega_k, a, T) \approx 50.35$ significantly smaller than $E(\omega_{(1/2)}, a = 25, T) \approx 1278.48$. This highlights the existence of several local minima. Actually, for this value, problem (P_ω) is ill-posed (see [25]) and the optimal domain is composed of an arbitrarily numbers of disjoint components distributed in ω: this phenomenon may be numerically detected by taking a sequence (in p) of initial guess $(\omega_{0,p})_{(p)}$ with an increasing number of disjoint components $\sharp\,\omega_{0,p}$: if the corresponding sequence $\sharp\,\omega_{k,p}$ - associated with the limit sequence of domain $(\omega_{k,p})_p$ - increases, then the ill-posedness is likely to hold.

5.1.3 Minimization with respect to both ω and $a(\boldsymbol{x})$

Using the algorithm (62), we now minimize the cost function with respect to both ω and a. According to our previous observations, these two variables are strongly coupled. We simply consider the case a constant in ω. Figure 15, associated with $(y_0, y_1) = (100\sin(\pi x_1)\sin(\pi x_2), 0.)$, depicts the limit of the zero-level set sequence $\{\boldsymbol{x} \in \Omega, \psi_k(\boldsymbol{x}) = 0\}$ obtained for different initializations ω_0 and $a_0 = 10.$ whereas Figure 16 depicts the evolution of a_k with respect to k. The results are summarized in Table 2. Except for $\omega_0 = \omega_{(0.35)}$ and $a_0 = 10.$ (see Fig 16 top left) leading to $E(\omega_k, a, T) \approx 140.12$, the minimization with respect to both ω and a leads to an impressive reduction of the cost function. Once again, the result depends on the initial values (ω_0, a_0) and is improved when ω_0 is composed of several disjoints parts. Finally, a better reduction is observed when the function a varies in ω.

Similar results are obtained with the viscous schemes (55) and (57).

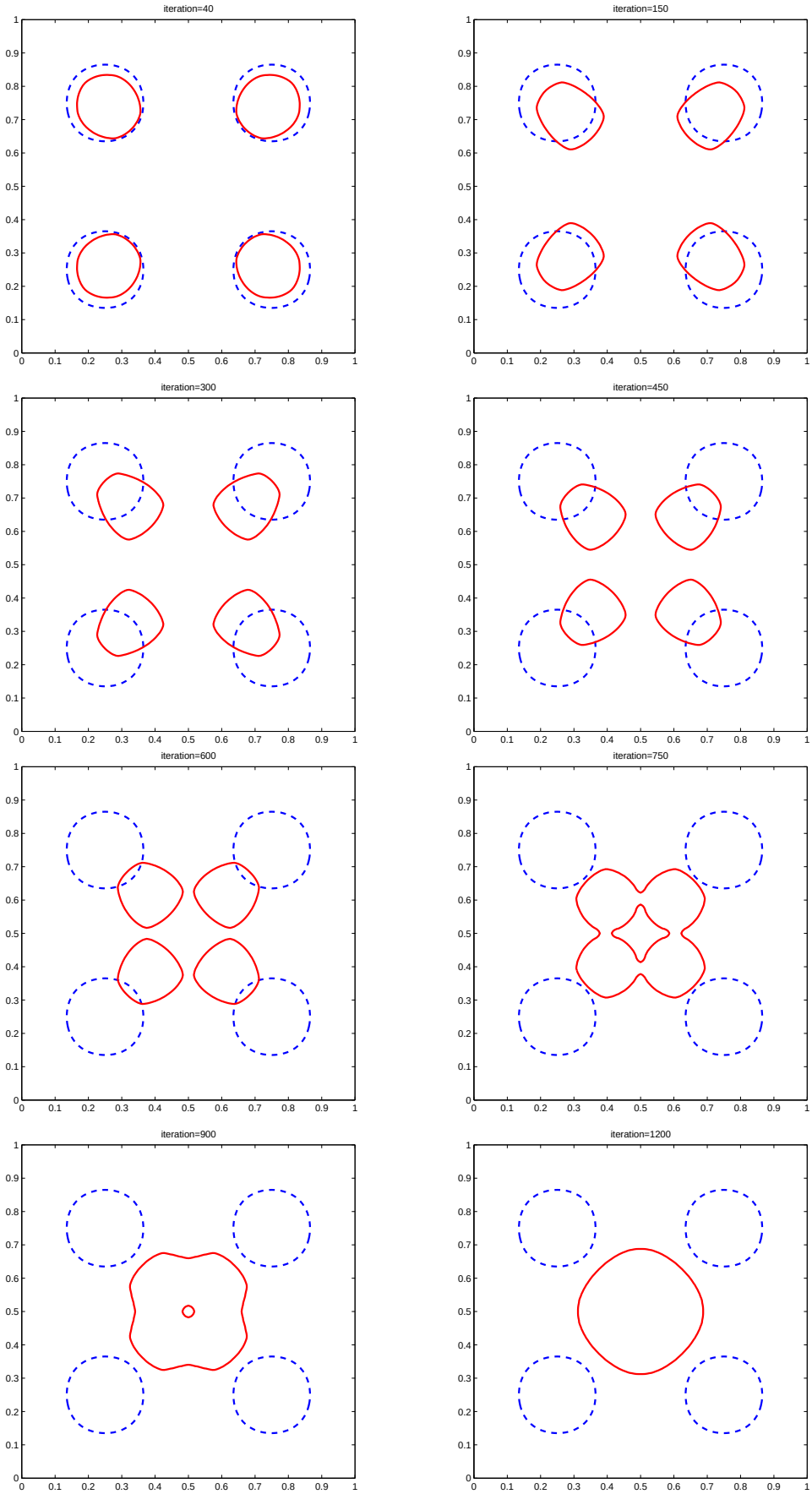

Figure 4: $(y_0, y_1) = (100\sin(\pi x_1)\sin(\pi x_2), 0)$, $T = 1$,$a = 10$. - Evolution of the zero-level set $\{\boldsymbol{x} \in \Omega, \psi_k(\boldsymbol{x}) = 0\}$ with respect to k.

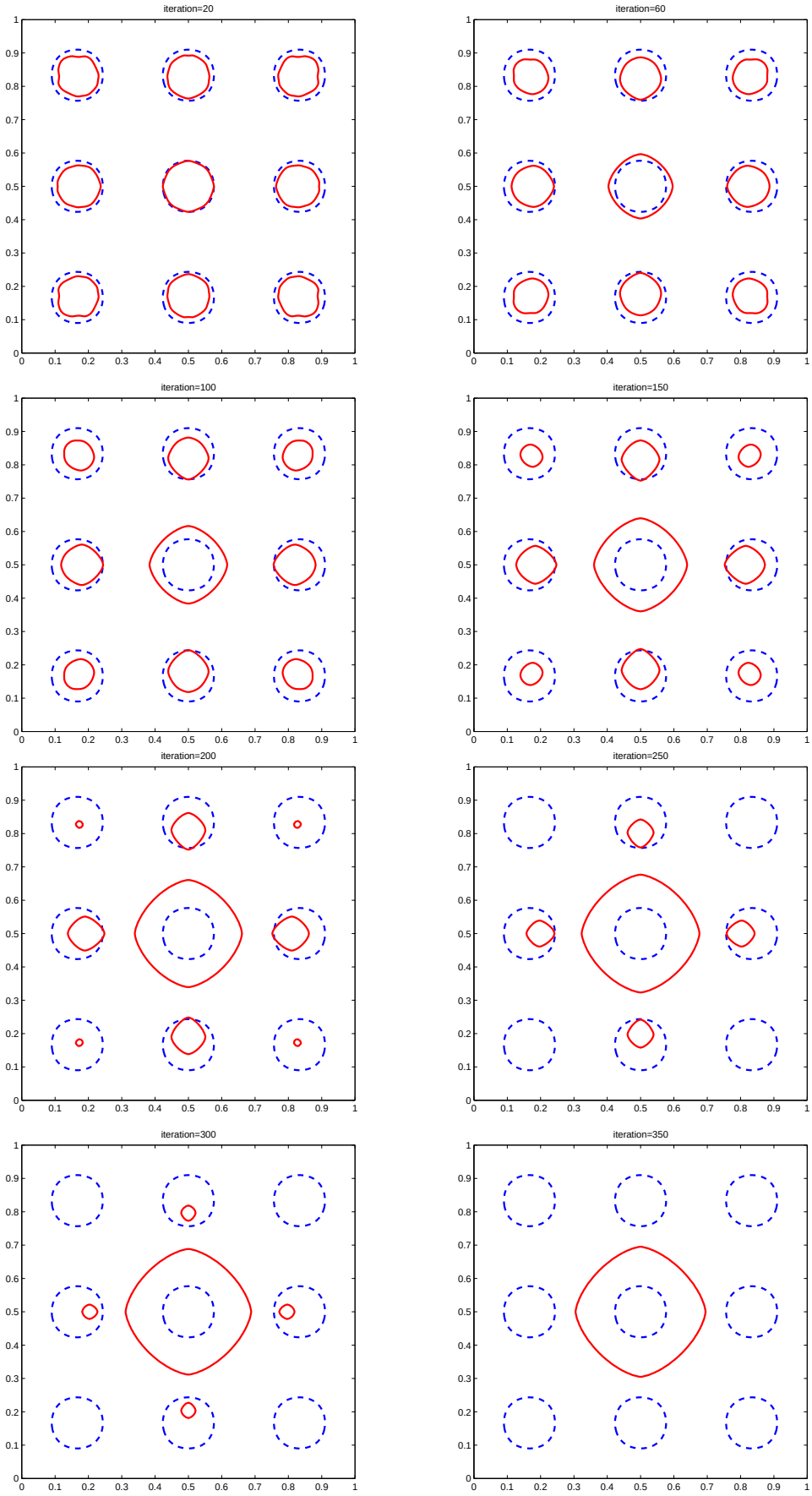

Figure 5: $(y_0, y_1) = (100\sin(\pi x_1)\sin(\pi x_2), 0)$, $T = 1$,$a = 10$. - Evolution of the zero-level set $\{\boldsymbol{x} \in \Omega, \psi_k(\boldsymbol{x}) = 0\}$ with respect to k.

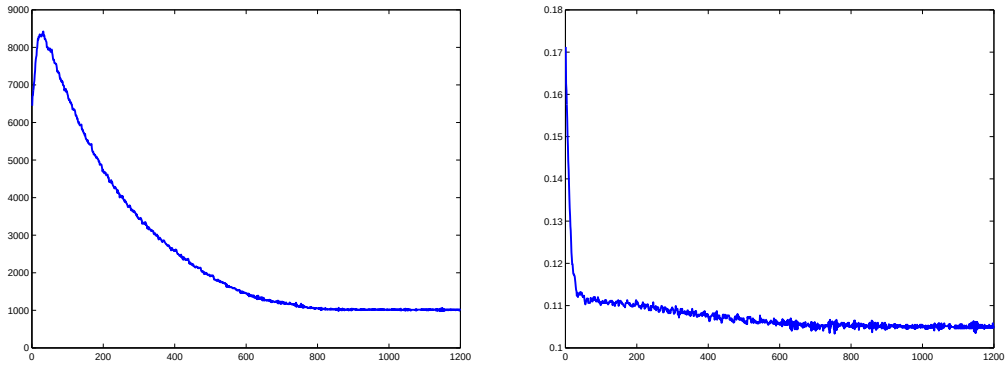

Figure 6: $(y_0, y_1) = (100\sin(\pi x_1)\sin(\pi x_2), 0)$, $T = 1$, $a = 10$. - Evolution of $E(\omega_k, a, T)$ (**Left**) and $|\omega_k|$ (**Right**) with respect to k (associated with Fig. 4).

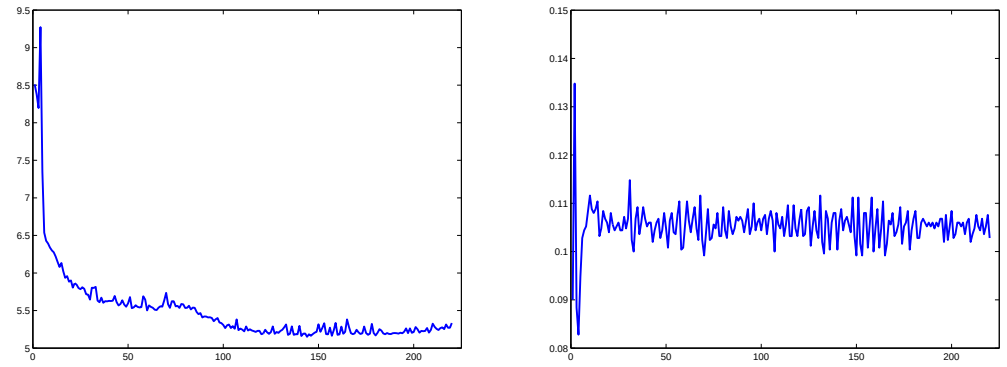

Figure 7: $(y_0, y_1) = (100\sin(\pi x_1)\sin(\pi x_2), 0)$, $T = 1$, $a = 10$. - Evolution of $E(\omega_k, a, T)$ (**Left**) and $|\omega_k|$ (**Right**) with respect to k (associated with Fig. 5).

	$\sharp\,\omega_0 = 1$	$\sharp\,\omega_0 = 4$	$\sharp\,\omega_0 = 16$	$\sharp\,\omega_0 = 49$
$E(\omega_{2000}, a_{2000}, 1)$	140.12	12.541	17.792	15.839
a_{2000}	19.51	29.098	35.122	29.38

Table 2: $E(\omega, a., T = 1)$ for different initial prediction ω_0 - $\sharp\,\omega_0$: number of disjoint parts of ω_0 - (associated with Fig. 15 and Fig. 16).

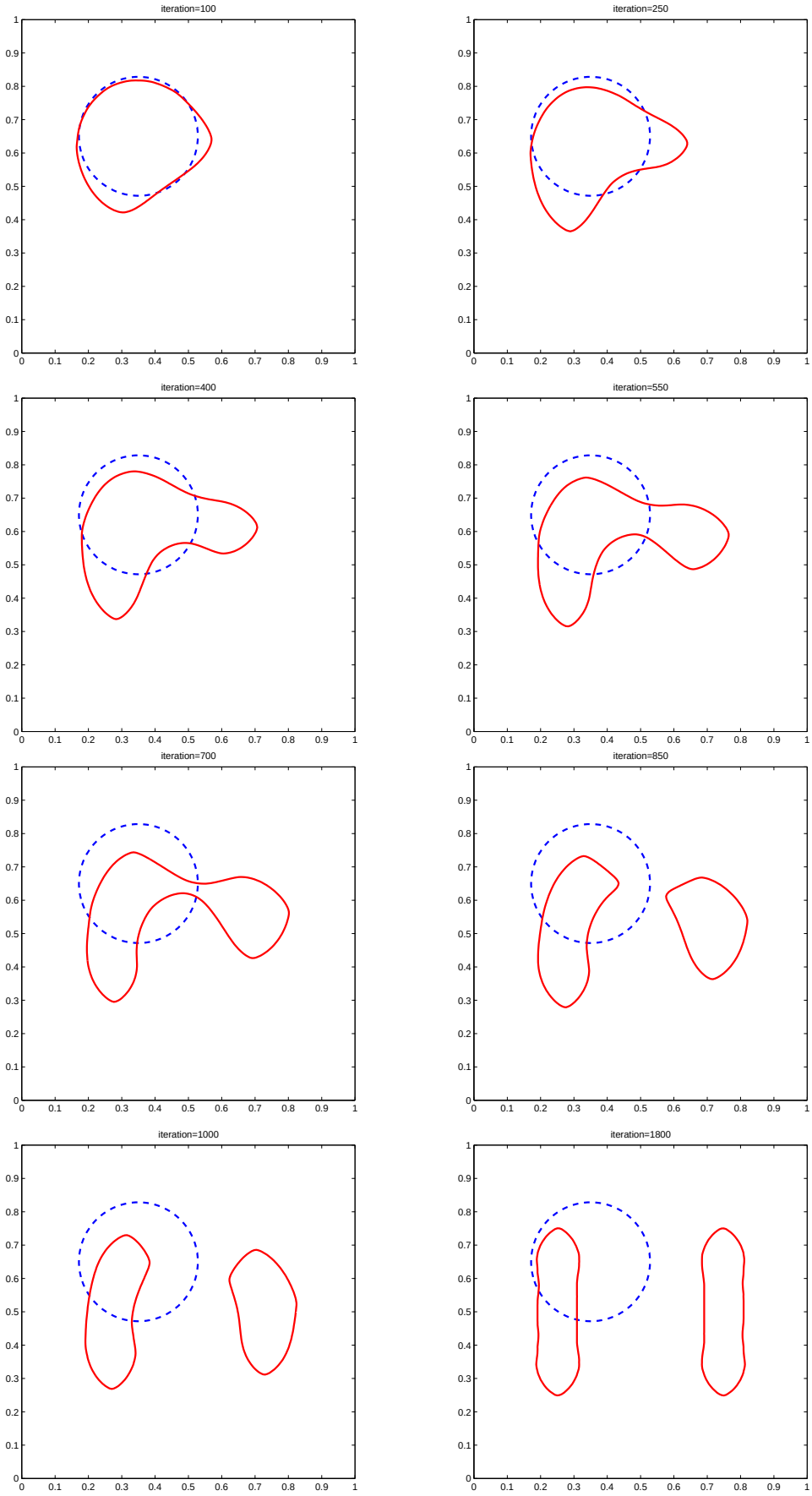

Figure 8: $(y_0, y_1) = (100 \sin(2\pi x_1) \sin(\pi x_2), 0)$, $T = 1$, $a = 10$. - Evolution of the zero-level set $\{\boldsymbol{x} \in \Omega, \psi_k(\boldsymbol{x}) = 0\}$ with respect to k.

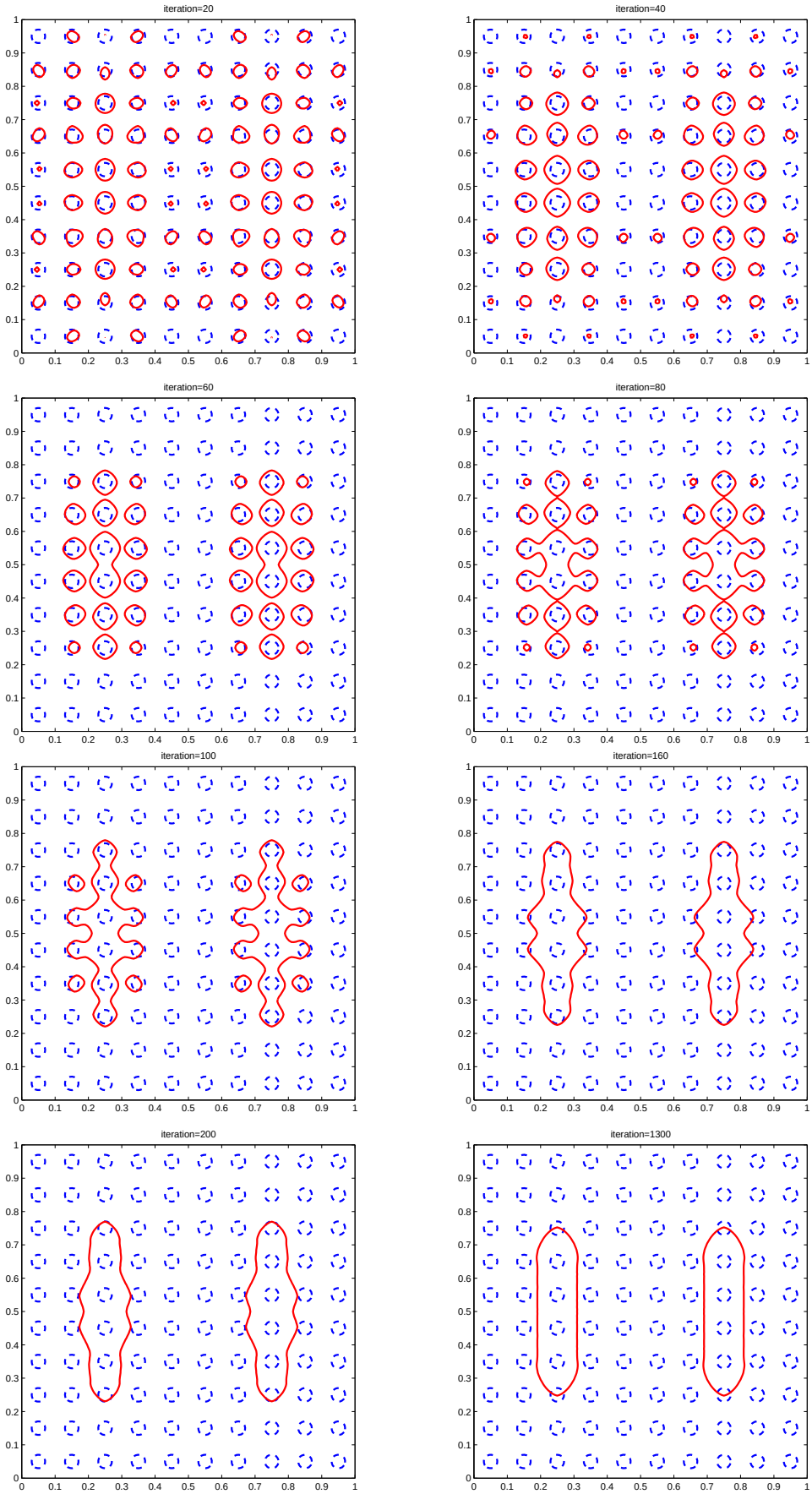

Figure 9: $(y_0, y_1) = (100 \sin(2\pi x_1) \sin(\pi x_2), 0)$, $T = 1$, $a = 10$. - Evolution of the zero-level set $\{\boldsymbol{x} \in \Omega, \psi_k(\boldsymbol{x}) = 0\}$ with respect to k.

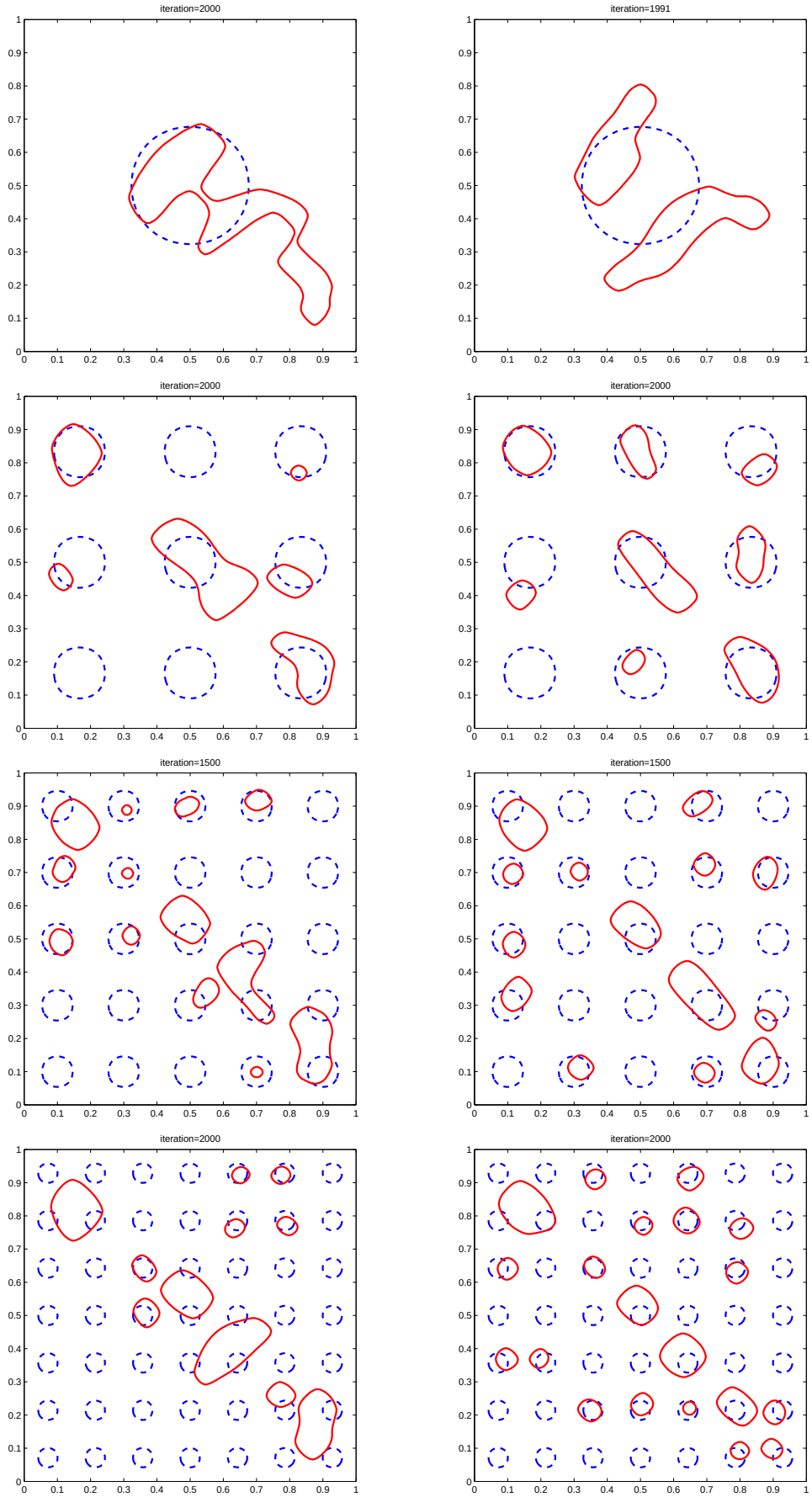

Figure 10: $(y_0, y_1) = (300x_1x_2(x_1-1)(x_2-1)\cos(5\pi x_1(x_2-1))\sin(2\pi x_1x_2), 0)$, $a = 10$. - "limit" of the sequence the zero-level set $\{\boldsymbol{x} \in \Omega, \psi_k(\boldsymbol{x}) = 0\}$ for different initial predictions of ω_0 - $T = 1$ (**Left**) and $T = 2$ (**Right**).

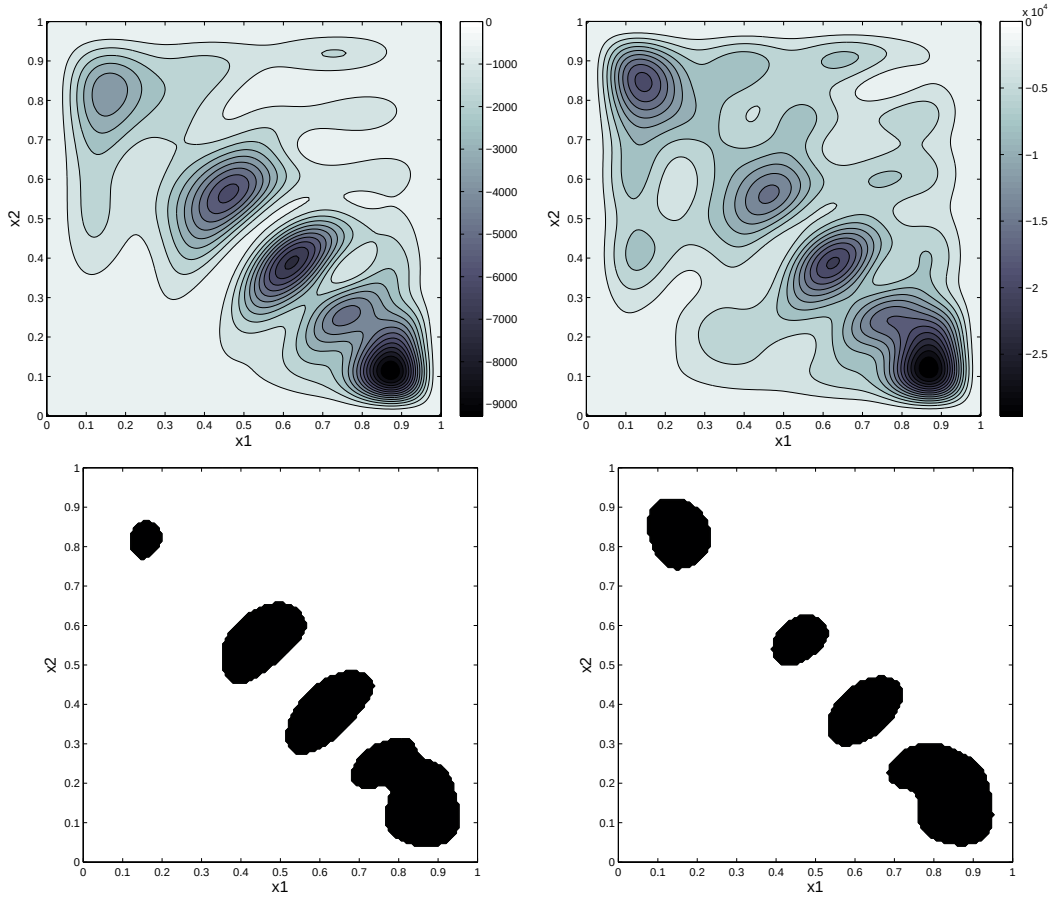

Figure 11: $(y_0, y_1) = (300x_1x_2(x_1-1)(x_2-1)\cos(5\pi x_1(x_2-1))\sin(2\pi x_1x_2), 0)$. Topological derivative $\boldsymbol{x} \to \int_0^T y'_{\emptyset,0}(\boldsymbol{x},t)p_{\emptyset,0}(\boldsymbol{x},t)dt$ in Ω (**Top**) and corresponding initialization ω_0 of size L (**Bottom**) - $T = 1$ (**Left**) and $T = 2$ (**Right**).

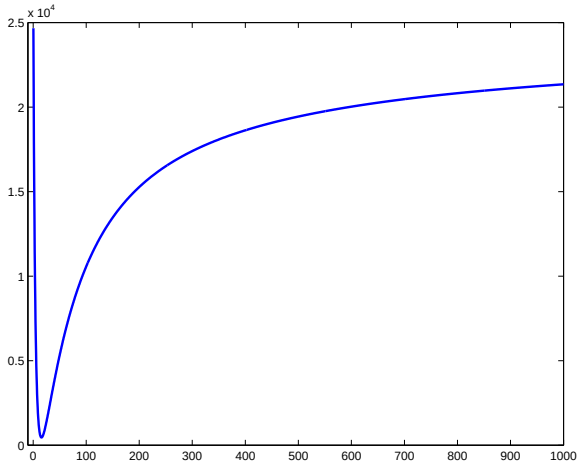

Figure 12: Illustration of the over-damping phenomenon when a is large -$E(\omega, a, T = 1)$ with respect to a (constant on ω) - ω is the disc of radius $\sqrt{0.1/\pi}$ centered on $(1/2, 1/2)$ - $E(\omega, 0, T) - E(\omega, a, T) \approx O(a^{-0.78})$, $a >> 1$.

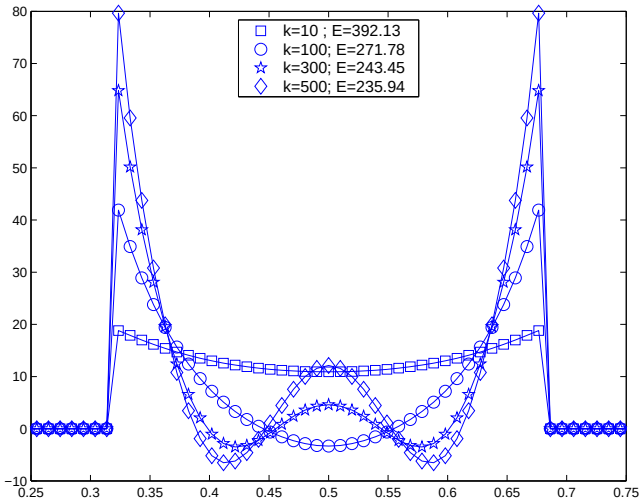

Figure 13: Optimization of $a(\boldsymbol{x})$ when ω is the disc of radius $\sqrt{L/\pi}$ centered on $(1/2, 1/2)$ - Graph of $a_k(x_1, x_2 = 1/2)$ along the axis (Ox_1) for different iterations.

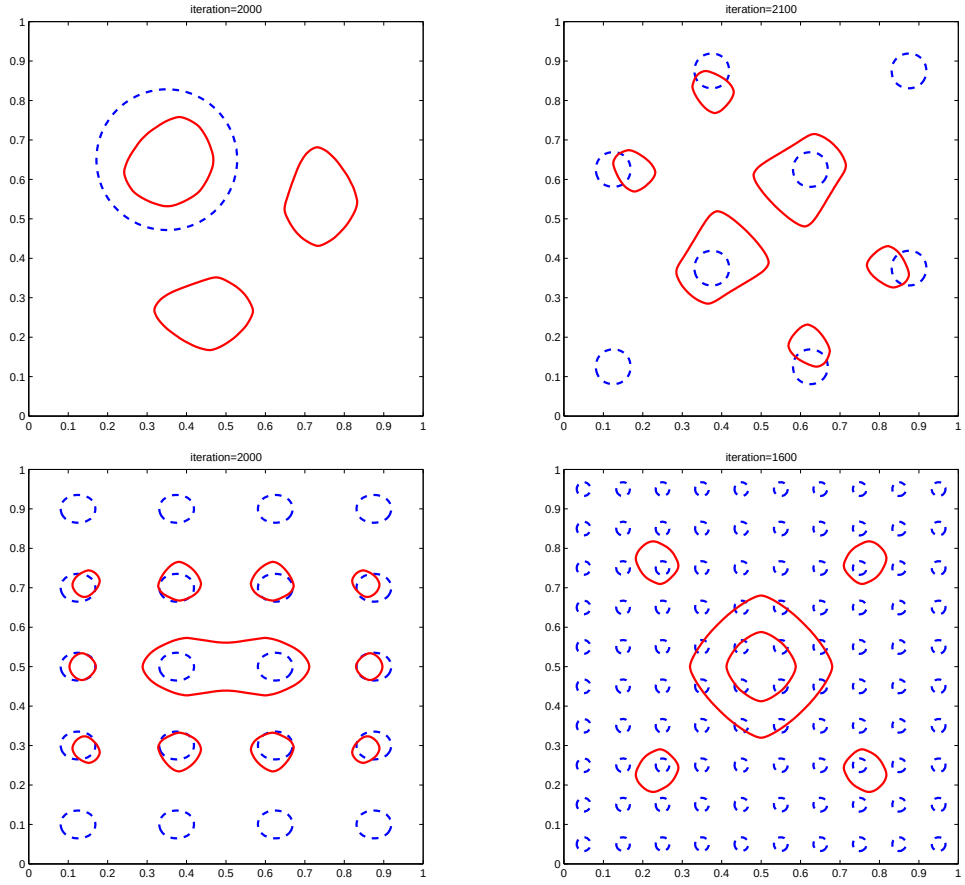

Figure 14: $(y_0, y_1) = (100 \sin(\pi x_1) \sin(\pi x_2), 0)$, $T = 1$, $a = 25$ - "limit" in k of the zero-level set sequence $\{\boldsymbol{x} \in \Omega, \psi_k(\boldsymbol{x}) = 0\}$ for different initial prediction ω_0. - top left: $E(\omega, a, T) = 101.08$ - top right: $E(\omega, a, T) = 93.47$ - bottom left: $E(\omega, a, T) = 34.82$ - bottom right: $E(\omega, a, T) = 50.35$.

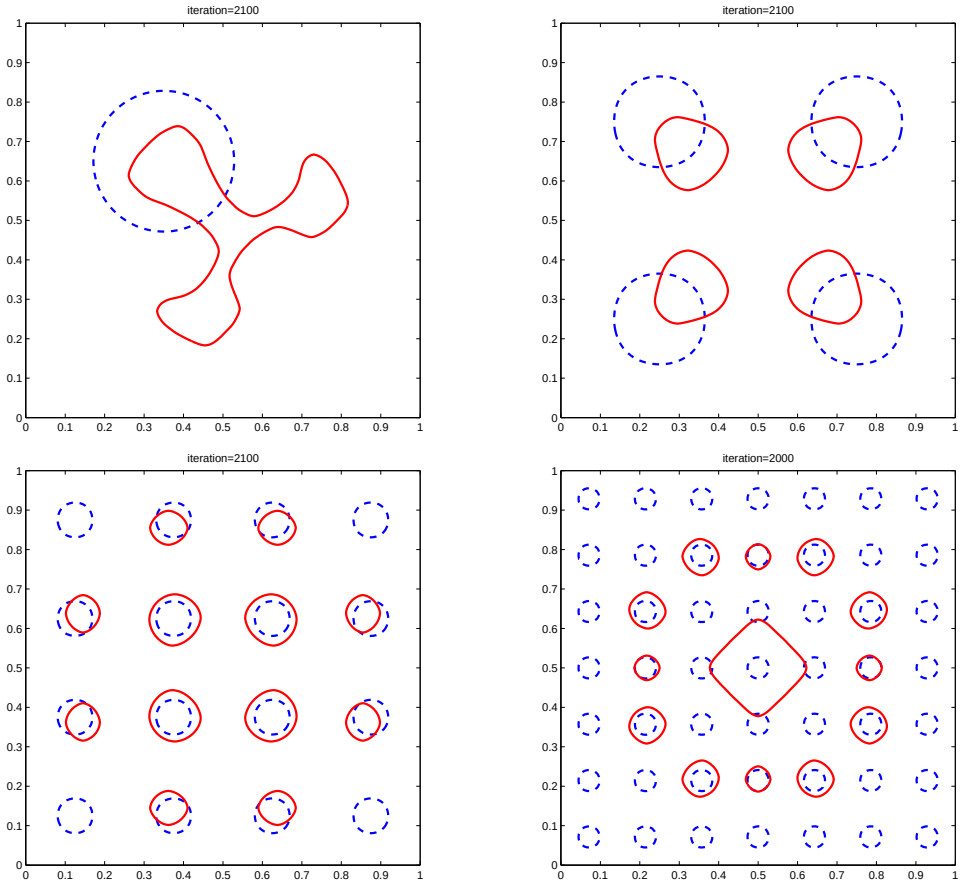

Figure 15: $(y_0, y_1) = (100 \sin(\pi x_1) \sin(\pi x_2), 0)$, $T = 1$- Optimization with respect to a and ω - "limit" of the sequence the zero-level set $\{\boldsymbol{x} \in \Omega, \psi_k(\boldsymbol{x}) = 0\}$ for four initial predictions ω_0.

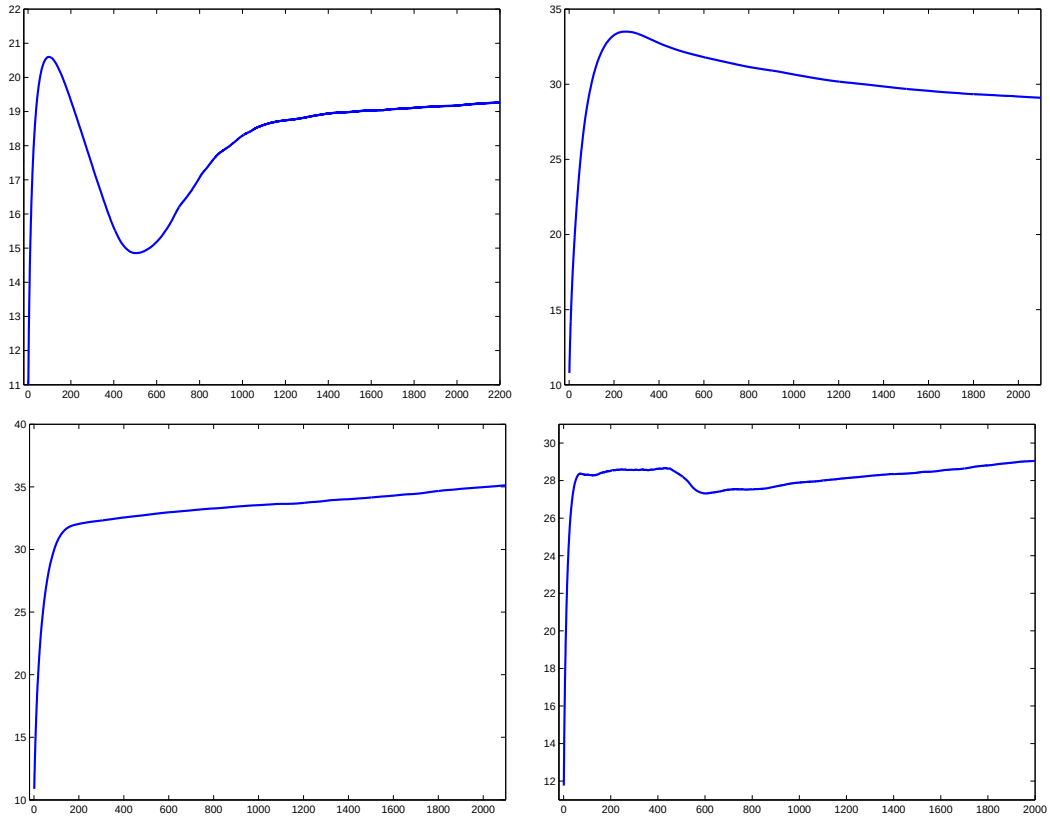

Figure 16: $(y_0, y_1) = (100\sin(\pi x_1)\sin(\pi x_2), 0)$, $T = 1$- Optimization with respect to a and ω - Evolution of a_k with respect to k associated with the initial prediction ω_0 of Fig. 15.

5.1.4 Interplay between the values of a and $|\omega|$ and topological derivative

The previous numerical simulation suggest that, for $|\omega|$ fixe, the problem (P_ω) is not well-posed as soon as a exceeds a critical value, says a_c. This critical value, depends, among others, on the size $|\omega|$. As already explained at the beginning of section 5.1.1, these points - related to the over-damping phenomenon - may be observed from the topological derivative. Let us consider the initial data (63), $L = |\omega| = 1/10$ and $T = 1$. According to the Section 5.1.1 and formula (37), if a is small enough, then the optimal position is the centered disc $D(\boldsymbol{x_0}, \rho) \subset \Omega$ for any ρ with $\boldsymbol{x_0} = (1/2, 1/2)$. Similarly, from the relation (34), if $|\omega|$ (equivalently ρ) is small enough, the disc $D(\boldsymbol{x_0}, \rho)$ is optimal for any value of a, so that a_c is a decreasing function of $|\omega|$. This bifurcation of the shape with respect to a may be detected from the computation of the topological derivative. Figure 17 displays the function $\boldsymbol{x} \to \int_0^T y'_{\omega,a}(\boldsymbol{x}, t) p_{\omega,a}(\boldsymbol{x}, t) dt$ for $\omega = D(\boldsymbol{x_0}, L/4)$ and two values of $a = 10$ (Left), $a = 25$ (Right). For $a = 10$, the derivative enforces the disc ω to increase smoothly (as expected) while for $a = 25$, the centered disc degenerates into a ring. For a large enough, ω is composed of an arbitrarily large number of disjoints components: such a structure may be obtained from a relaxation procedure (we refer to [25]).

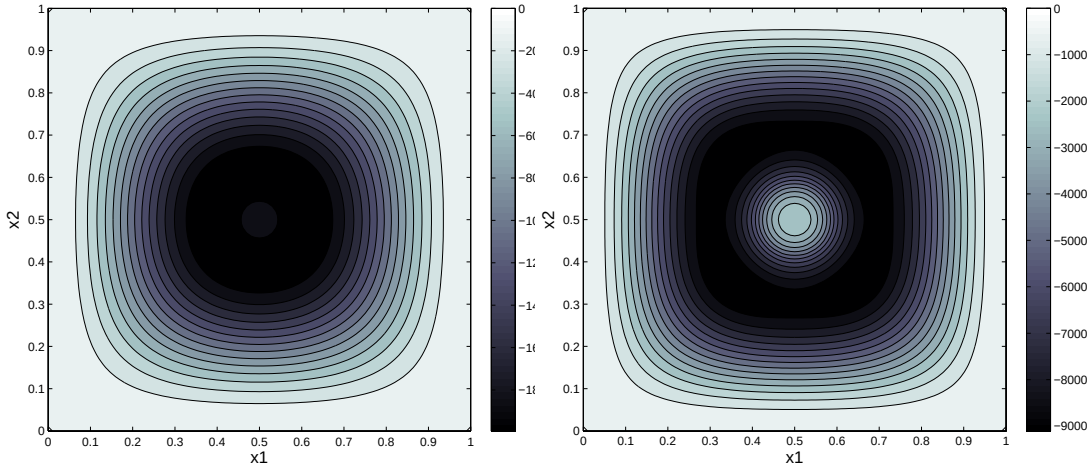

Figure 17: $(y_0, y_1) = (100 \sin(\pi x_1) \sin(\pi x_2), 0)$, $T = 1$-

5.2 Irregular initial conditions

So far, we have considered regular initial condition (y_0, y_1) for which - at the numerical level - the use of viscosity terms is unnecessary. In order to highlight the importance of the high frequency component on the mechanism of dissipation, let us consider the most singular situation with a discontinuous initial condition y_0. We give only one example and refer to [16] in 1-D. On the unit square $\Omega = (0, 1)^2$, we define

$$y_0(\boldsymbol{x}) = \begin{cases} 40 & (x_1, x_2) \in (\frac{1}{3}, \frac{2}{3})^2 \\ 0 & \text{elsewhere} \end{cases} \quad ; \quad y_1(\boldsymbol{x}) = 0, \tag{66}$$

$a(\boldsymbol{x}) = 10.\, \mathcal{X}_\omega(\boldsymbol{x})$ and then optimize with respect to ω. Figure 18 displays the limit in k the boundary of ω_k obtained respectively with the usual schemes without viscosity terms and with the modified viscous schemes (55)-(57). The limit is different and we observe that the modified scheme leads to an energy significantly lower (see Figure 19). Without viscosity terms, we obtain $E(\omega, a, T) \approx 2768.70$ whereas with viscosity terms, we obtain

$E(\omega, a, T) \approx 1487.23$. Once again, in spite of the symmetry of y_0, the centered disc $\omega_{(1/2)}$ of area L is not the optimal domain: we compute $E(\omega_{(1/2)}, a, T) \approx 1984.72$.

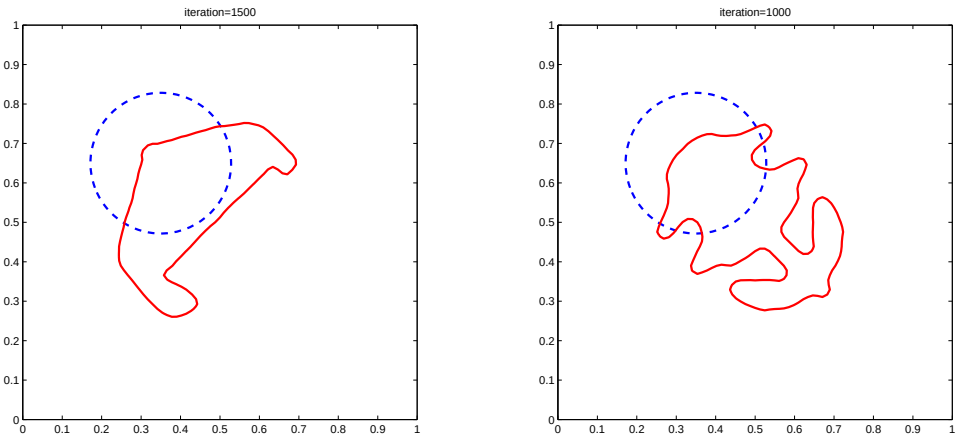

Figure 18: Singular case. $T = 1$, $a = 10$ - "limit" in k of the zero-level set sequence $\{\boldsymbol{x} \in \Omega, \psi_k(\boldsymbol{x}) = 0\}$ without viscosity terms $E(\omega, a, T) \approx 2768.70$ (**Left**) and with viscosity terms $E(\omega, a, T) = 1487.23$ (**Right**).

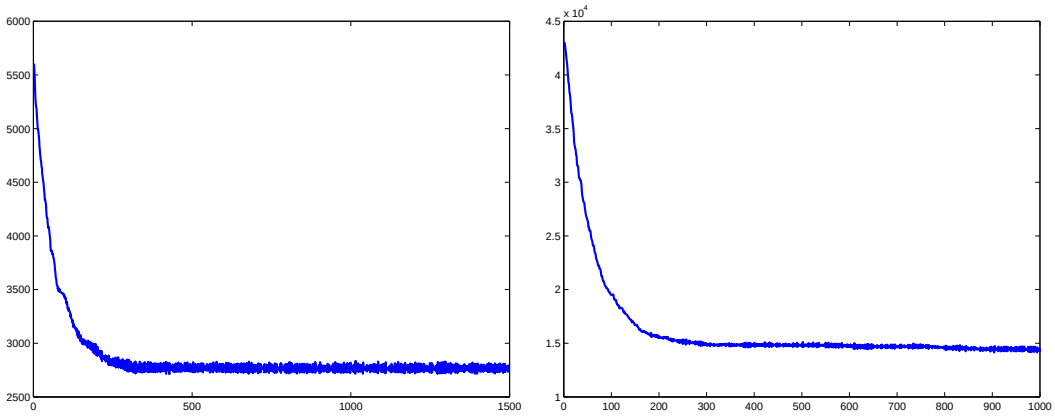

Figure 19: Singular case. $T = 1$, $a = 10$ - Energy $E(\omega_k, a, T = 1)$ with respect to k without (**Left**) and with (**Right**) viscosity terms.

6 Concluding remarks

We have numerically solved the shape design problem which consists in optimizing the support of a damped term for the linear wave equation. This work completes the previous theoretical study performed in [25] where a well-posed relaxation for (P_ω) is derived. In agreement with [25], the numerical experiments highlights the crucial influence of the over-damping phenomenon on the optimal position. On the one hand, when the damping coefficient is small enough (this depends on the data of the problem), problem (P_ω) is well-posed: the topological derivative then provides a good approximation of the design, improved iteratively by the level set method. On the other hand, when the damping coefficient is large, the problem is ill-posed and the algorithm yields to local optima. First, this illustrates the

complexity and richness of the problem in contrast to the apparent simplicity of the linear system. Secondly, this also emphasizes the efficiency of this descent method coupled with a level set approach to detect or not local minima. Moreover, when the support is fixed, the dissipation is optimized with high gradient and locally negative damping function. Once again, this result, in agreement with the literature, is due to the over-damping phenomenon.

The case of the boundary dissipation may be numerically analyzed in a similar way as well as others models such as piezo-elastic systems [10]. In the context of exact controllability for the wave equation wave, we refer to [23] where the optimal shape of the control is analyzed. Finally, adapting [21] and [32], it seems interesting and challenging to analyze the non-cylindrical situation where the support ω may depend on time.

References

[1] Allaire G., Jouve F., Toader A.M., *Structural optimization using sensitivity analysis and a level-set method*, J. Comp. Phys., **194(1)**, 363-393 (2004).

[2] Allaire G., de Gournay F., Jouve F., Toader A.M., *Structural optimization using topological and shape sensitivity analysis via a level-set method*, Control. Cybernet., **34(1)**, 59-80 (2005).

[3] Banks H.T., Ito K., Wang B., *Exponentially stable approximations of weakly damped wave equations*, Ser. Num. Math. **100**, 1-33, Birkhäuser (1990).

[4] Bardos C., Lebeau G., Rauch J., *Sharp sufficient conditions for the observation, control and stabilization from the boundary*, SIAM J. Control and Opt., **30**, 1024-1065 (1992).

[5] Burger M., Osher S.J., *A survey on level set methods for inverse problems and optimal design*, European Journal of Applied Mathematics, **16(2)**, 263-301 (2005).

[6] Cagnol J., Zolesio J.P., *Shape derivative in the wave equation with Dirichlet boundary condition*, J. Diff. Eq **158**, 175-210, (1999).

[7] Castro C., Cox S.J., *Achieving arbitrarily large decay in the damped wave equation*, Siam J. Control Optim. **6**, 1748-1755, (2001).

[8] Cohen G.C., *Higher-order Numerical Methods for Transient Wave Equations*, Scientific Computation, Springer, (2002).

[9] Delfour M.C., Zolesio J.P., *Shapes and Geometries - Analysis, Differential Calculus and Optimization*, Advances in Design and Control, SIAM, (2001).

[10] Degryse E., Mottelet S., *Shape optimization of piezoelectric sensors or actuators for the control of plates*, Control, Optimization and Calculus of Variation, **4** 673-690 (2005).

[11] Fahroo F., Ito K., *Variational formulation of optimal damping designs*, Contemporary Math., **209**, 95-114 (1997).

[12] Freitas P., *Optimizing the rate of decay of solutions of the wave equation using genetic algorithms : a counterexample to the constant damping conjecture*, Siam J. Control. Optim., **37**, 376-387 (1998).

[13] Fulmanski P., Laurain A., Scheid J-F., Sokolowski J., *Level set method with topological derivatives in shape optimization*, Int. J. of Computer Mathematics, To appear.

[14] Glowinski R., Kinton W., Wheeler M.F., *A mixed finite element formulation for the boundary controllability of the wave equation*, Int. J. Numer. Methods. Eng., **27**, 623-636 (1989).

[15] Hebrard P., Henrot A., *Optimal shape and position of the actuators for the stabilization of a string*, Systems and control letters, **48**, 199-209 (2003).

[16] Hebrard P., Henrot A., *A spillover phenomenon in the optimal location of actuators*, Siam J. Control and Optimization, **44**, 349-366 (2005).

[17] Henrot A., Maillot H., *Optimization of the shape and the location of the actuators in an internal control problem*, Boll. Unione Mat. Ital. Sez. B Artic. Ric. Mat., **3**, 737-757 (2001).

[18] Henrot A., Pierre M., *Variation et Optimisation de formes - Une analyse géométrique*, Mathématiques et Applications **48**, 334 p. (2005).

[19] Lions J.L., Magenes E., *Problèmes aux limites non homogènes et applications, vol. 1*, Dunod, Paris (1968).

[20] López-Gómez J., *On the linear damped wave equation*, J. Differential Equations **134**, 26-45, (1997).

[21] Maestre F., Münch A., Pedregal P., *A spatio-temporal design problem for a damped wave equation*, SIAM on Journal Applied Mathematics **68**, 109-132, (2007).

[22] Münch A., *A uniformly controllable and implicit scheme for the 1-D wave equation*, Mathematical Modelling and Numerical Analysis **39**, 377-418, (2005).

[23] Münch A., Optimal design of the support of the control for the 2-D wave equation : numerical investigations, International Journal of Numerical Analysis and Modeling, **5**, 331-351 (2008).

[24] Münch A., Pazoto A., *Uniform stabilization of a numerical approximation of the locally damped wave equation*, Control, Optimization and Calculus of Variation, **13**, 265-293 (2007).

[25] Münch A., Pedregal P., Periago P., *Optimal design of the damping set for the stabilization of the wave equation*, Journal of Differential Equation, **231(1)**, 331-358 (2006).

[26] Münch A., Pedregal P., Periago P., *Optimal internal stabilization of the linear system of elasticity*. To appear in Archive Rational Mechanical analysis. (2008).

[27] Osher S.J., Sethian J.A., *Fronts propagating with curvature-dependent speed: algorithms based on Hamilton-Jacobi formulations*, J. Comput. Phys., **79**, 12-49 (1988).

[28] Sokolowski J., Zochowski A., *On the topological derivative in shape optimization*, SIAM J. Control Optim., **37**, 1251-1272 (1999).

[29] Osher S.J., Fedkiw R., *Level set methods and dynamics implicit surfaces*, Applied Mathematics Sciences, Springer-Verlag, **153**, (2002).

[30] Sethian J.A., *Level set methods: Evolving interfaces in geometry, fluid mechanics, computer vision, and materials science*, Cambridge University Press, (1996).

[31] Wang M.Y., Wang X., Guo D., *A level set method for structural topology optimization*, Computat. Methods. Appl. Mech. Engrg. **192**, 227-246, (2003).

[32] Zolésio J.P., Truchi C., *Shape stabilization of wave equation*, Lecture Notes in Control and Information Sciences, J.P. Zolesio editor **100** 372-398, (1987) .